

Flexible joint models for multivariate longitudinal and time-to-event data using multivariate functional principal components

Alexander Volkmann^{*1}, Nikolaus Umlauf², and Sonja Greven¹

¹*Chair of Statistics, School of Business and Economics, Humboldt-Universität zu Berlin, Germany*

²*Department of Statistics, Faculty of Economics and Statistics, Universität Innsbruck, Austria*

Abstract

The joint modeling of multiple longitudinal biomarkers together with a time-to-event outcome is a challenging modeling task of continued scientific interest. In particular, the computational complexity of high dimensional (generalized) mixed effects models often restricts the flexibility of shared parameter joint models, even when the subject-specific marker trajectories follow highly nonlinear courses. We propose a parsimonious multivariate functional principal components representation of the shared random effects. This allows better scalability, as the dimension of the random effects does not directly increase with the number of markers, only with the chosen number of principal component basis functions used in the approximation of the random effects. The functional principal component representation additionally allows to estimate highly flexible subject-specific random trajectories without parametric assumptions. The modeled trajectories can thus be distinctly different for each biomarker. We build on the framework of flexible Bayesian additive joint models implemented in the R-package ‘bamlss’, which also supports estimation of nonlinear covariate effects via Bayesian P-splines. The flexible yet parsimonious functional principal components basis used in the estimation of the joint model is first estimated in a preliminary step. We validate our approach in a simulation study and illustrate its advantages by analyzing a study on primary biliary cholangitis.

1 Introduction

More and more medical studies are gathering information on their participants’ longitudinal profiles of different biomarkers together with the time to an event of interest such as rejection of a transplanted organ [10], onset of a disease [13], or death [33]. It is then of interest to model the longitudinal profiles together with the time-to-event data to gain a detailed understanding of the association of the different processes and to improve prediction for new subjects.[8, 54, 38] Shared parameter models are a popular approach to jointly modeling the longitudinal and time-to-event processes.[35] They typically combine mixed effects models for the longitudinal data with a hazard model for the time-to-event data through shared random effects. For multiple longitudinal outcomes, however, the generalized mixed models and thus the shared parameter models can become quite computationally expensive due to a large number of parameters to estimate. This can restrict the flexibility with which the longitudinal outcomes are modeled, even though the respective longitudinal trajectories often exhibit strong non-linearities in practice.[35, 19, 22] Recent research has thus focused on lowering the computational costs of these multivariate joint models (MJMs) by adapting two-stage methods (fitting the longitudinal submodel and using its output to fit the time-to-event submodel)[28, 29], improving numerical efficiency[36], or using approximate expectation-maximization algorithms[31, 32] or approximate Bayesian methods[44, 47].

Here, we propose a further means of reducing the computational complexity of MJMs, which can be combined with the aforementioned approaches. By understanding the longitudinal profiles as functions over the follow-up time, we introduce multivariate functional principal component analysis (MFPCA) as a popular tool for dimension reduction in functional data analysis to the MJM framework. This allows us to represent the shared random effects using multivariate functional principal components (MFPCs), which has several advantages: An MFPCs basis representation allows to model highly flexible functional random effects while being parsimonious at the same time. These basis functions efficiently capture correlated nonlinear trends over the different longitudinal outcomes, thus admitting a flexible modeling approach with relatively few parameters, especially compared to a (penalized) spline approach for each longitudinal outcome. As the MFPCA decomposes the entire multivariate random process, the number of MFPC based random effects needed for a good model fit does not directly depend on the number of longitudinal outcomes but only on the complexity of the covariance structure. Furthermore, the MFPCs form an orthogonal basis with uncorrelated random weights (due to the Karhunen-Loève theorem), which simplifies the generally unstructured random effects covariance matrix of e.g. random spline basis coefficients to a diagonal matrix. Finally, the MFPCs can be ordered by the amount of

variation they explain, which provides a handy criterion for further dimension reduction by dropping relatively unimportant modes of variation from the estimation and thus reducing the number of parameters in the model.

There is a wide range of work that has combined functional data analysis with joint models of (multivariate) longitudinal and time-to-event outcomes. Some of this work has focused on incorporating functional data such as images as baseline covariates or as a repeatedly measured longitudinal functional outcome.[59, 23, 21, 24, 60, 18, 61] In this context, the functional domain is different from the follow-up time and functional principal component analysis is used to achieve a low dimensional representation of the functional data. Here, we propose to view repeated scalar measurements as functional data so that the functional domain coincides with the follow-up time. This has also been considered by other authors, particularly in the context of two-stage models and dynamic predictions.[16, 55, 56, 25, 17, 27, 7] These approaches use univariate functional principal component analysis (UFPCA) or MFPCA to estimate principal components and scores for the longitudinal submodel and plug the scores into the survival submodel. While two-stage approaches are known to yield biased parameter estimates[46, 40], the previously mentioned works show that this estimation bias does not necessarily negatively affect the predictive performance. Other approaches simultaneously estimate the principal components and scores within the univariate[57] or multivariate joint model.[26, 22] For multiple longitudinal outcomes, however, these proposed MJMs feature strong assumptions. Li et al. (2021)[26] use UFPCA to model a common latent trajectory shared by all longitudinal outcomes, which allows to represent only highly correlated markers. Li et al. (2022)[22] and Zou et al. (2023)[62] extend this approach by further including outcome specific latent trajectories, but assume them to be independent and identically distributed (i.i.d.) across outcomes and subjects. In both approaches, the dependence between longitudinal outcomes is explained by only one shared latent factor, which might not be adequate for multiple biomarkers from potentially different biological pathways.

While our proposed estimation approach also involves two steps, it is important to note that this differs greatly from the previously mentioned two-stage procedures. In the preliminary step, we estimate MFPCs via MFPCA. These are then used as an empirical, flexible, and parsimonious basis to model the multiple longitudinal outcomes within an MJM, thus incorporating the time-to-event information together with the longitudinal modelling and avoiding estimation bias induced by the marginal two-stage approach. Volkman et al. (2023)[51] show that this two step estimation process using estimated MFPCs works well and provides the flexibility to fit complex multivariate functional data. We are thus extending their work to the scenario where the multivariate functional data are subject to informative missingness.

Our implementation combines the flexibility and parsimoniousness of using an MFPC basis representation of functional random effects with the framework of flexible additive joint models proposed by Köhler et al. (2017)[19]. This framework incorporates the shared parameter models into Bayesian additive models for location, scale, and shape[48], and provides versatile, powerful, and easy to use modeling options for covariate effects. The implementation allows to include for example smooth, linear, spatial, time-varying, or random effects terms of one or more covariates in the longitudinal and time-to-event submodels, using the well developed and documented architecture of the R package **mgcv**[52] for generalized additive models[53]. This supports more (and arguably easier to use) options for the specification of nonlinear covariate effects than other available R software[15, 12, 30], in particular the popular **JMbayes2** package[43]. We adopt a derivative based Markov chain Monte Carlo (MCMC) algorithm to estimate the full MJM, thus avoiding the different proposed approximations such as via two-stage approaches as in Mauff et al. (2020)[28].

We illustrate our proposed approach by analyzing a well known and publicly available primary biliary cholangitis (PBC) data set[40]. It is based on a study conducted by the Mayo Clinic from January 1974 to May 1984 on the survival of patients with PBC (previously called primary biliary cirrhosis), which is a rare chronic liver disease causing the inflammation and destruction of small bile ducts.[33] This data set is still widely used in recent literature [1, 31, 32, 34, 44, 47], mainly due to two reasons: it is one of the last studies to allow the analysis of the natural history of PBC patients treated only with supportive care [9] and it features an interesting data structure. Several biochemical measurements are available for 312 subjects at different time points after entering the study, with missing observations and dropout due to censoring, liver transplantation, or death. Furthermore, these longitudinal measurements have previously been found to follow non-linear trajectories and to be associated with the patients' survival.[1, 20, 44] Using an MFPCs based representation of the random effects can lower the computational burden while increasing the flexibility in the modeling of the longitudinal trajectories, which can lead to a more accurate estimation of the association between the longitudinal and the event processes.

This paper is structured as follows. Section 2 formally introduces the flexible MJM as well as the MFPC representation of the random effects, while Section 3 presents the proposed estimation of the MFPC basis and the flexible MJM. In Section 4 we examine our approach in different simulation scenarios and illustrate its applicability using the PBC data in Section 5. Section 6 closes with a discussion and outlook.

2 Methodology

In the following, we present a flexible joint model for multivariate longitudinal outcomes and time-to-event data. We follow and extend the notation of Köhler et al. (2017)[19] to emphasize the high flexibility of all model parts as structured additive predictors, including modeling nonlinear covariate effects using Bayesian P-splines. We then introduce the idea of representing the shared random effects of the joint model using multivariate functional principal components, which gives a parsimonious representation of a possibly very complex covariance structure.

2.1 Multivariate joint model

Let $T_i \in \mathcal{I}$ denote the potentially right-censored event time for subject $i = 1, \dots, n$ with $\mathcal{I} = [0, T_{max}]$ and T_{max} the maximal follow-up time. We model the hazard $h_i(t)$ of an event for subject i at time $t \in \mathcal{I}$ as a function of K longitudinally observed markers and further covariates as

$$h_i(t) = \exp\{\eta_i(t)\} = \exp\{\eta_{\lambda_i}(t) + \eta_{\gamma_i} + \sum_{k=1}^K \eta_{\alpha_k i}(t) \cdot \eta_{\mu_k i}(t)\}, \quad (1)$$

where $\eta_i(t)$ is a structured additive predictor for subject i at time t given a set of baseline and time-dependent covariates \mathbf{x}_i . Note that we suppress the dependency on t for the set of covariates for better readability. The additive predictor $\eta_i(t)$ can be further separated into structured additive predictors $\eta_{\lambda_i}(t)$ for the baseline hazard, time-dependent covariates, and time-dependent covariate effects, η_{γ_i} for the baseline covariates, and the possibly time-dependent association modeled by $\eta_{\alpha_k i}(t)$ of the hazard with the K longitudinal outcomes $\eta_{\mu_k i}(t)$, $k = 1, \dots, K$. We consider the “true” underlying longitudinal outcomes $\eta_{\mu_k i}(t)$ as structured additive functions over \mathcal{I} and assume them to be square-integrable, $\eta_{\mu_k i}(t) \in L^2(\mathcal{I})$. These functions, however, are only observed at subject and outcome specific time-points $t_{ijk}, j = 1, \dots, n_{ik}$ with corresponding longitudinal observations y_{ijk} modeled as

$$y_{ijk} = \eta_{\mu_k i}(t_{ijk}) + \epsilon_{ijk}, \quad (2)$$

where ϵ_{ijk} represents independent Gaussian noise

$$\epsilon_{ijk} \stackrel{\text{ind}}{\sim} N(0, \exp\{\eta_{\sigma_k i}(t_{ijk})\}^2), \quad (3)$$

whose variance depends on the structured additive predictor $\eta_{\sigma_k i}(t_{ijk})$.

The association predictors $\eta_{\alpha_k i}(t)$ link the multivariate longitudinal submodel of equations (2) and (3) to the time-to-event submodel (1). The resulting MJM connects the current outcome levels to the risk of experiencing the event at time t . Note that we estimate separate association predictors $\eta_{\alpha_k i}(t)$ for the different longitudinal predictors $\eta_{\mu_k i}(t)$, allowing us to identify longitudinal outcomes important for the time-to-event process.

The additive predictors

$$\eta_l(t) = \sum_{h=1}^{H_l} f_{lh}(\mathbf{x}_i, t), l \in \mathcal{L} := \{\lambda, \gamma, \alpha_1, \dots, \alpha_K, \mu_1, \dots, \mu_K, \sigma_1, \dots, \sigma_K\}$$

comprise parametric or nonparametric functions of \mathbf{x}_i as well as random effects, all potentially varying over time t . In particular, the effects $f_h(\mathbf{x}_i, t)$ depend on subsets of covariates in \mathbf{x}_i ; they can specify linear or smooth covariate effects of single covariates in \mathbf{x}_i or interaction effects of two or more such covariates. As an illustration, a scalar, time-constant covariate $z_i \in \mathbf{x}_i$ might be modeled as having a linear effect $z_i \cdot \beta$, a linear effect varying over time $z_i \cdot f(t)$, a smooth effect $f(z_i)$, or a smooth effect over time $f(z_i, t)$. For a detailed overview of different possible effect specifications including spatial or covariate interaction effects, see Table 2 of Köhler et al. (2017)[19]. We use suitable basis representations such as spline basis matrices with corresponding penalties to model the structured additive predictors as explained in detail in Section 3.2. In particular, we further separate the longitudinal predictors

$$\eta_{\mu_k i}(t) = \sum_{h=1}^{H_{\mu_k} - 1} f_{kh}(\mathbf{x}_i, t) + b_i^{(k)}(t) \quad (4)$$

into outcome specific (functional, i.e. potentially time-varying) fixed effects $f_{kh}(\mathbf{x}_i, t) \in L^2(\mathcal{I}), h = 1, \dots, H_{\mu_k} - 1$, and subject and outcome specific functional random effects $b_i^{(k)}(t)$, which account for the correlation of longitudinal outcome values within a subject over time and across different markers.[45, 51] To model this correlation structure, we assume that the multivariate functional random effects $\mathbf{b}_i(t) = (b_i^{(1)}(t), \dots, b_i^{(K)}(t))^T \in L_K^2(\mathcal{I})$ with $L_K^2(\mathcal{I}) = L^2(\mathcal{I}) \times \dots \times L^2(\mathcal{I})$ are independent copies of a smooth zero-mean Gaussian random

process with multivariate covariance kernel \mathcal{K} . The associated covariance operator $\Gamma : L_K^2(\mathcal{I}) \rightarrow L_K^2(\mathcal{I})$ given by $(\Gamma \mathbf{g})(t) = \langle \langle \mathbf{g}, \mathcal{K}(t, \cdot) \rangle \rangle$ is based on the (potentially weighted) scalar product

$$\langle \langle \mathbf{g}, \mathbf{h} \rangle \rangle := \sum_{k=1}^K w_k \int_{\mathcal{I}} g^{(k)}(t) h^{(k)}(t) dt, \quad \mathbf{g}, \mathbf{h} \in L_K^2(\mathcal{I}) \quad (5)$$

for given positive weights $w_k, k = 1, \dots, K$, inducing a Hilbert space structure[14]. Setting weights unequal to one allows to let variation from different longitudinal outcomes contribute differently to the multivariate kernel, which will be discussed in more detail in Section 3.1. The corresponding covariance surfaces $\mathcal{K}^{(d,e)}(s, t) = \text{Cov} [b_i^{(d)}(s), b_i^{(e)}(t)]$, $d, e = 1, \dots, K$ and $s, t \in \mathcal{I}$, are auto-covariances for $d = e$ and cross-covariances for $d \neq e$.

The auto-covariances describe the correlation structure of the random effects within a longitudinal outcome. The covariance implied by a subject specific constant shift and linear time trend such as in a parametric random intercept – random slope mixed model would be contained as a special case. We do not parametrically restrict the auto-covariance structure, however, and it can thus also represent more flexible nonparametric forms such as in Köhler et al. (2017)[19]. The cross-covariances capture the correlation structure between the different longitudinal outcomes. As these are hard to realistically specify a priori, especially for nonparametric random effects, we allow the cross-covariances to nonparametrically vary with the pair of time-points considered. Furthermore, we assume the $\mathbf{b}_i(t)$ to be independent of the Gaussian noise process (3), which allows to separate the error variance from the diagonal of the smooth covariance kernel \mathcal{K} . [58]

2.2 Functional principal component representation of random effects

Köhler et al. (2017)[19] achieve a flexible (auto-)covariance structure for one longitudinal marker by representing the functional random effects using B-spline basis functions with random effect weights. For multiple longitudinal outcomes, however, such an approach can become prohibitive as the number of parameters quickly increases: Using D basis functions for each $b_i^{(k)}(t)$ results in $n \cdot K \cdot D$ random basis weights with a $(K \cdot D) \times (K \cdot D)$ unstructured covariance matrix Σ containing $(K \cdot D + 1)K \cdot D/2$ unknown parameters. Given that the desired flexibility is in practice often achieved by penalizing a large number D of basis coefficients, a resulting MJM suffers from the considerable number of parameters to estimate. On the other hand, reducing the number D or assuming a diagonal covariance matrix, or both, are simplifying but unrealistic assumptions which could impair the estimation of the association with the event hazard.

Instead, we propose to use a functional principal components based representation of the multivariate functional random effects. We apply the multivariate Karhunen-Loève (KL) theorem[14], which allows to represent multivariate functional data in an infinite basis expansion using random scores and the eigenfunctions of the corresponding covariance operator. For the multivariate functional random effects we get

$$\mathbf{b}_i(t) = \sum_{m=1}^{\infty} \rho_{im} \psi_m(t) \approx \sum_{m=1}^M \rho_{im} \psi_m(t) \quad (6)$$

with random scores ρ_{im} and the eigenfunctions $\psi_m(t) = (\psi_m^{(1)}(t), \dots, \psi_m^{(K)}(t))^{\top} \in L_K^2(\mathcal{I})$ of the covariance kernel \mathcal{K} [14, 51], i.e. due to Mercer's theorem $\mathcal{K}(s, t) = \sum_{m=1}^{\infty} \nu_m \psi_m(s) \psi_m(t)^{\top}$ with ordered eigenvalues $\nu_1 \geq \nu_2 \geq \dots \geq 0$. Note that the eigenfunctions $\psi_m, m = 1, \dots, \infty$ are orthonormal to each other with respect to the scalar product (5). The scores $\rho_{im} \sim (0, \nu_m)$ are uncorrelated across m and, in particular, for the Gaussian process $\mathbf{b}_i(t)$ are i.i.d. $\rho_{im} \sim N(0, \nu_m)$. In practice, the infinite expansion in (6) is truncated at a finite level using the leading M eigenfunctions, where the truncation order M controls the approximation accuracy. This truncated multivariate KL representation has several benefits: Interpretability, dimension reduction, and the simplification of the scalar random effects covariance matrix to a diagonal matrix.

The leading eigenfunctions correspond to the main modes of variation in the data due to decreasing corresponding eigenvalues and can be interpreted as outcome specific characteristic trajectories corresponding to correlated patterns that are simultaneously present across all longitudinal outcomes. The direction and strength of expression of these characteristic trajectories for each subject depend on their individual score ρ_{im} . The eigenvalues ν_m corresponding to the eigenfunctions allow to quantify their contributions to the overall variation in the data given that $E(\langle \langle \mathbf{b}_i, \mathbf{b}_i \rangle \rangle) = \sum_{k=1}^K w_k \int_{\mathcal{I}} \text{Var}(b_i^{(k)}(t)) dt = \sum_{m=1}^{\infty} \nu_m$. This can be used to determine the quality of the approximation in (6), e.g. by choosing M such that a pre-specified large percentage of variation is retained. We estimate the eigenfunctions as MFPCs in a preliminary step described in section 3.1, leaving only the random scores ρ_{im} to be estimated as random effects in the MJM. This considerably reduces the number of parameters from $n \cdot K \cdot D$ to $n \cdot M$: The scores act as weights for multivariate functions and are thus not outcome-specific. In addition, M only depends on the complexity of the covariance kernel \mathcal{K} , which is not necessarily connected to the number of longitudinal outcomes K , such that typically in practice $M \ll K \cdot D$. Using the orthonormal MFPCs as basis functions for the Gaussian random process also leads to

i.i.d. $\boldsymbol{\rho}_i = (\rho_{i1}, \dots, \rho_{iM})^\top \sim N_M(\mathbf{0}, \text{diag}(\nu_1, \dots, \nu_M))$, $i = 1, \dots, n$, where the mean of the M -dimensional multivariate normal distribution is the vector of zeros $\mathbf{0}$ and the covariance matrix is diagonal with eigenvalues ν_m as elements. This represents a further simplification, reducing the covariance parameters to $M \ll (K \cdot D + 1)K \cdot D / 2$ independent of K , and implies computational advantages compared to an unstructured covariance matrix $\boldsymbol{\Sigma}$ of a B-spline approach as described above.

The eigenfunction based representation of the random effects gives the best (in terms of integrated squared error [39]) approximation to the longitudinal outcomes $\mathbf{b}_i(t)$ for a given number of basis functions and allows a parsimonious model formulation. While in practice we have to use estimates of the basis functions $\boldsymbol{\psi}_m(t)$ in the MJM, we are less interested in the MFPCs themselves, although they provide additional interpretations of main directions of variation in marker trajectories. Our simulations show that even imperfectly estimated versions still serve as a good empirical basis for the longitudinal trajectories and give the MJM the flexibility needed for a good model fit, yielding better results than more restrictive parametric or spline-based approaches in settings with nonlinear trends over time.

3 Estimation

We use a derivative-based MCMC algorithm adapted from the one for univariate joint models proposed by Köhler et al. (2017)[19] to estimate the posterior distribution of the parameter vector $\boldsymbol{\theta}$ containing all model parameters of interest in a Bayesian framework. Note that the MFPC basis is estimated directly from the data and is thus not part of $\boldsymbol{\theta}$. This might be interpreted as an empirical Bayes approach; however, we prefer to view the MFPCs simply as a beneficial empirical basis for the random effects (comparable to e.g. pre-defined B-spline basis functions). The following sections outline the estimation of the MFPC basis and the Bayesian estimation of $\boldsymbol{\theta}$.

3.1 Estimation of the MFPC basis

We estimate the MFPC basis following the MFPCA proposed by Happ and Greven (2018)[14], which estimates the multivariate covariance kernel \mathcal{K} from separate UFPCAs based on the different longitudinal outcomes of each subject. This approach is very flexible as it allows to specify the UFPCA for each longitudinal outcome individually and relies only on the covariance between the estimated univariate scores of the subjects.

In a first step, we estimate a mean trajectory $\eta_{\mu_k}^*(t_{ijk})$ for each longitudinal outcome using the outcome specific fixed effects $\sum_h^{H_{\mu_k} - 1} f_{kh}(\mathbf{x}_i, t)$ specified for the MJM under a working independence assumption for the longitudinal observations ignoring censoring. We then estimate the auto-covariance of each longitudinal outcome $y_{ijk}(t) \in L^2(\mathcal{I})$ as a bivariate surface using fast symmetric additive covariance smoothing based on the crossproducts of the centered longitudinal observations $y_{ijk}^* = y_{ijk} - \eta_{\mu_k}^*(t_{ijk})$. [5] A truncated eigendecomposition of the covariance surface then yields estimates for the first M_k univariate eigenfunctions $\phi_{km_k} \in L^2(\mathcal{I})$ and eigenvalues corresponding to the variances of the scores $\xi_{km_k i}$ in the univariate KL expansion $y_{ijk}(t) \approx \eta_{\mu_k}^*(t) + \sum_{m_k=1}^{M_k} \xi_{km_k i} \phi_{km_k}(t)$. Given the estimated principal components $\hat{\phi}_{km_k}$, the univariate scores $\xi_{km_k i}$ are predicted using a conditional expectation approach. [58] Other approaches of estimating the UFPCA are also possible (cf. Section 6).

For a Hilbert space induced by (5), Happ and Greven (2018)[14] show that the multivariate eigenfunctions are given as linear combinations of their univariate counterparts and derive the explicit formula for this relationship as $\boldsymbol{\psi}_m^{(k)}(t) = (w_k)^{-1/2} \sum_{m_k=1}^{M_k} c_{km_k} \phi_{km_k}(t)$, with linear combination weights c_{km_k} depending on (the eigenvectors of) the covariance matrix of the univariate scores $\xi_{km_k i}$, $k = 1, \dots, K$. [14] The MFPCA thus uses the estimated covariance structure of the estimated univariate scores of all longitudinal outcomes to estimate the MFPCs and consequently the multivariate covariance kernel \mathcal{K} . Regarding the choice of weights in (5), setting $w_1 = \dots = w_K = 1$ can be a reasonable starting point for the analysis in many cases. When the range or variation of the longitudinal data differ considerably between the longitudinal outcomes, we propose to use weights inversely proportional to the integrated univariate variance as given by the sum of univariate eigenvalues from the UFPCAs. [14] This approach is equivalent to standardization of the different longitudinal markers to make them comparable, as commonly also done in non-functional multivariate principal component analysis, while avoiding rescaling of the data. The resulting MFPCs are then often more balanced across the longitudinal outcomes, avoiding MFPCs which are dominated by one longitudinal outcome essentially capturing variation of that outcome alone. Refraining from the rescaling of longitudinal outcomes has the additional advantage that the association structure of the MJM via the current value of the longitudinal outcomes can be interpreted much more intuitively.

As the MFPC basis is an important part of the subsequent MJM, its estimation should be closely monitored in practice. It is important that the UFPCAs are flexible enough to capture all the relevant modes of variation in the data. In particular, the univariate truncation order M_k should be high and a sufficient number of

basis functions for the estimation of the univariate covariance surface should be specified, as variation lost by oversmoothing on the univariate level is lost for all later stages of the analysis. In addition, the penalization chosen by the fast symmetric additive covariance smoothing directly influences the smoothness of the MFPCs and consequently also the final fit of the MJM. Visually inspecting the estimated MFPC basis and consulting a subject matter expert about their beliefs on systematic variation in the data at this stage of the analysis can be helpful.

Note that the estimation of the MFPC basis uses the estimated covariance between the estimated univariate scores. As univariate scores are estimated with large uncertainty if only very few longitudinal observations are available, we recommend a trimmed approach where we use all longitudinal observations of subjects with at least one measurement after 10% of the time interval \mathcal{I} on all longitudinal outcomes. In our experience, this approach avoids extremely outlying estimates of univariate scores in the UFPCA for subjects with very early censoring, which via the estimated covariance between the univariate scores can have a detrimental effect on the estimated MFPC basis. Alternatively, outlying scores can be manually identified and removed from the MFPCA, or robust alternatives to trimming such as weighting would also be possible.

Given a reasonable estimate of the MFPC basis, the multivariate eigenvalues ν_m of the MFPCA can be used to choose the truncation order M of the multivariate functional random effects representation (6). The maximal number $M^* = \sum_{k=1}^K M_k$ of MFPCs corresponds to the total number of univariate functional principal components (UFPCs) in the MFPCA. Reducing $M < M^*$ allows further dimension reduction for the parameter vector $\boldsymbol{\theta}$ with relatively little loss in the estimation quality for high M as shown in Section 4. A common criterion is to use a threshold for the ratio of cumulative explained variance, e.g. 99%, and discard all trailing MFPCs. Given the MFPC basis, choosing M thus reduces to a model selection problem and can also be solved using standard approaches such as comparing information criteria for different model fits.

3.2 Basis representation of effects

The proposed MJM is very flexible with respect to the readily available types of covariate effects for all structured additive predictors $\eta_{li}(t) = \sum_{h=1}^{H_l} f_{lh}(\mathbf{x}_i, t)$, $l \in \mathcal{L}$. The Bayesian additive mixed models framework allows a wide range of effects such as linear, smooth, or random effects terms by using corresponding basis function expansions for $f_{lh}(\mathbf{x}_i, t)$ combined with associated priors.[48] All of these flexible effects, including the functional principal component based random effects, can be represented in matrix notation as

$$\mathbf{f}_{lh} = \mathbf{X}_{lh}\boldsymbol{\beta}_{lh} \quad (7)$$

with vector \mathbf{f}_{lh} of stacked function evaluations over all subjects for the survival submodel (vector length n) or over all subjects, markers and time points for the longitudinal submodel (vector length $N = \sum_i \sum_k n_{ik}$), design matrix \mathbf{X}_{lh} , and coefficient vector $\boldsymbol{\beta}_{lh}$. This representation includes but is not limited to non-linear covariate effects, which can be represented as such a matrix product with the columns of \mathbf{X}_{lh} containing e.g. evaluations of spline basis functions. For the representation of further model terms, see Umlauf et al. (2018)[48] and Köhler et al. (2017)[19]. Note that standard sum-to-zero constraints are used to center the design matrix \mathbf{X}_{lh} of non-linear functions[45, 53] in order to ensure model identifiability in a model also including an intercept.

In particular, the functional principal components based random effects $b_i^{(k)}(t)$ for one longitudinal outcome in (4) can be expressed as

$$\mathbf{b}^{(k)} = \mathbf{X}_{\mu_k H_{\mu_k}} \boldsymbol{\beta}_{\mu_k H_{\mu_k}} = \text{blockdiag}(\boldsymbol{\Psi}_1^{(k)}, \dots, \boldsymbol{\Psi}_n^{(k)}) \boldsymbol{\rho}, \quad (8)$$

where the $N_k = \sum_i n_{ik}$ -vector $\mathbf{b}^{(k)}$ contains the evaluations of the subject and outcome specific functional random effect at the observed time points for outcome k and all objects i and $\boldsymbol{\rho} = (\boldsymbol{\rho}_1^\top, \dots, \boldsymbol{\rho}_n^\top)^\top$ is the vector containing M random scores $\boldsymbol{\rho}_i$ per subject (corresponding to the coefficient vector $\boldsymbol{\beta}_{\mu_k H_{\mu_k}}$). The design matrix $\mathbf{X}_{\mu_k H_{\mu_k}}$ has a blockdiagonal structure with blocks $\boldsymbol{\Psi}_i^{(k)}$ per i , which is an $n_{ik} \times M$ matrix containing evaluations of the k -th component of the M MFPCs at time points t_{ijk} , $j = 1, \dots, n_{ik}$. Note that $\boldsymbol{\rho}$ is not specific to outcome k and its dimension thus does not scale with K due to our dimension reduction approach. Consequently, stacking the longitudinal outcomes to $\mathbf{b} = (\mathbf{b}^{(1)\top}, \dots, \mathbf{b}^{(K)\top})^\top$ simply corresponds to stacking the K blockdiagonal design matrices to a full multivariate longitudinal design matrix $\mathbf{X}_{\mu H_{\mu}} = (\mathbf{X}_{\mu_1 H_{\mu_1}}^\top, \dots, \mathbf{X}_{\mu_K H_{\mu_K}}^\top)^\top$ with a single coefficient vector $\boldsymbol{\rho}$. We point out that using a standard (spline) random effects basis for \mathbf{b} would not be as parsimonious. While for each k the design matrix $\mathbf{X}_{\mu_k H_{\mu_k}}$ would have a similar blockdiagonal structure as in (8) with blocks containing the evaluations of the random effect (spline) basis, the random coefficient vector $\boldsymbol{\beta}_{\mu_k H_{\mu_k}}$ would be different for each k . As a result, combining the longitudinal outcomes would be equivalent to constructing a full multivariate longitudinal design matrix $\mathbf{X}_{\mu H_{\mu}} = \text{blockdiag}(\mathbf{X}_{\mu_1 H_{\mu_1}}, \dots, \mathbf{X}_{\mu_K H_{\mu_K}})$.

3.3 Priors

In order to achieve the penalization of flexible effects in a Bayesian setting, appropriate priors for β_{lh} are specified. In general, we assume multivariate normal priors

$$p(\beta_{lh} | \tau_{lh}^2) \propto (\tau_{lh}^2)^{-\frac{\text{rank}(\mathbf{K}_{lh})}{2}} \exp\left(-\frac{1}{2\tau_{lh}^2} \beta_{lh}^\top \mathbf{K}_{lh} \beta_{lh}\right) \quad (9)$$

with variance parameter τ_{lh}^2 , $\text{rank}(\mathbf{A})$ denoting the rank of matrix \mathbf{A} , and \mathbf{K}_{lh} the chosen precision matrix. The variance parameter takes the role of an inverse smoothing parameter controlling the trade-off between flexibility and smoothness of the flexible effect, while the precision matrix determines the type of penalization and contains e.g. difference penalties for Bayesian P-splines.[48] We assume independent inverse Gamma hyperpriors for the variance parameters $\tau_{lh}^2 \sim IG(0.001, 0.001)$, which results in inverse Gamma full conditionals but other priors, such as half-Cauchy, are also possible. Furthermore, priors for anisotropic smooths containing multiple variance parameters can be specified as given in Köhler et al. (2017) [19]. For linear or parametric time-constant terms, we approximate $\mathbf{K}_{lh} = \mathbf{0}$ by using $\beta_{lh} \sim N(\mathbf{0}, 1000^2 \mathbf{I})$ with identity matrix \mathbf{I} .

Following the truncated KL representation (6), we can assume independent random scores over the subjects i and the MFPCs m so that we can separate $\boldsymbol{\rho} = (\boldsymbol{\rho}_{(1)}, \dots, \boldsymbol{\rho}_{(M)})^\top$ with $\boldsymbol{\rho}_{(m)} = (\rho_{1m}, \dots, \rho_{nm})^\top$ and use separate priors for each $\boldsymbol{\rho}_{(m)}$. In particular, we assume the multivariate normal priors (9) for each m , with precision matrix $\mathbf{K}_{(m)} = \mathbf{I}$ and different variance parameters $\tau_{(m)}^2$. Note that the variances $\tau_{(m)}^2$ correspond to the eigenvalues ν_m in the MFPCA. We emphasize viewing the estimated MFPCs as an empirical basis by using the above introduced weak Gamma priors for the $\tau_{(m)}^2$ instead of using the estimated eigenvalues ν_m in the priors. With our specification, the ρ_{im} take the role of random effects for the basis functions ψ_m - defined simultaneously for all k on the entire follow-up time interval \mathcal{I} - as a flexible data-driven basis, replacing parametric basis functions such as e.g. a constant and a linear function per k in a random intercept - random slope model.

3.4 Likelihood

We use the standard assumption of shared random effects models that given the parameter vector $\boldsymbol{\theta}$, the longitudinal outcomes $\mathbf{y} = (\mathbf{y}_1^\top, \dots, \mathbf{y}_K^\top)^\top$ and the survival outcome $[\mathbf{T}, \boldsymbol{\delta}]$ are conditionally independent. Here, $\mathbf{y}_k = (\mathbf{y}_{1k}^\top, \dots, \mathbf{y}_{nk}^\top)^\top$, $\mathbf{y}_{ik} = (y_{i1k}, \dots, y_{in_{ik}k})^\top$, $\mathbf{T} = (T_1, \dots, T_n)^\top$ the follow-up (event or censoring) times, and the event indicators $\boldsymbol{\delta} = (\delta_1, \dots, \delta_n)^\top$ are 1 if the subject experiences the event and 0 for censoring. This allows to factorize the likelihood of the MJM as the product of the Likelihood L^{surv} of survival submodel (1) and the Likelihood L^{long} of the longitudinal submodel (2)-(3). The log-likelihood of the MJM can then be formulated as

$$\ell(\boldsymbol{\theta} | \mathbf{T}, \boldsymbol{\delta}, \mathbf{y}) = \ell^{surv}(\boldsymbol{\theta} | \mathbf{T}, \boldsymbol{\delta}) + \ell^{long}(\boldsymbol{\theta} | \mathbf{y}) \quad (10)$$

with the log-likelihoods ℓ^{surv} and ℓ^{long} of the survival and longitudinal submodels, respectively.

For the survival submodel, the log-likelihood can be expressed as

$$\ell^{surv}(\boldsymbol{\theta} | \mathbf{T}, \boldsymbol{\delta}) = \boldsymbol{\delta}^\top \boldsymbol{\eta}(\mathbf{T}) - \mathbf{1}_n^\top \boldsymbol{\Lambda}(\mathbf{T}),$$

where $\boldsymbol{\eta}(\mathbf{T}) = (\eta_1(T_1), \dots, \eta_n(T_n))^\top$, $\mathbf{1}_u$ is the u -vector of ones, and $\boldsymbol{\Lambda}(\mathbf{T}) = (\Lambda_1(T_1), \dots, \Lambda_n(T_n))^\top$ is the vector of cumulative hazard rates $\Lambda_i(T_i) = \int_0^{T_i} \eta_i(s) ds$.

The log-likelihood of the longitudinal submodel is similar to a multivariate functional additive mixed model [51] with the longitudinal outcomes stacked in the outcome vector \mathbf{y} and

$$\ell^{long}(\boldsymbol{\theta} | \mathbf{y}) = -\frac{N}{2} \log(2\pi) - \mathbf{1}_N^\top \boldsymbol{\eta}_\sigma - \frac{1}{2} (\mathbf{y} - \boldsymbol{\eta}_\mu)^\top \mathbf{R}^{-1} (\mathbf{y} - \boldsymbol{\eta}_\mu)$$

with similarly stacked vectors $\boldsymbol{\eta}_\sigma = (\boldsymbol{\eta}_{\sigma_1}^\top, \dots, \boldsymbol{\eta}_{\sigma_K}^\top)^\top$, $\boldsymbol{\eta}_{\sigma_k} = (\boldsymbol{\eta}_{\sigma_{k1}}^\top, \dots, \boldsymbol{\eta}_{\sigma_{kn}}^\top)^\top$, $\boldsymbol{\eta}_{\sigma_{ki}} = (\eta_{\sigma_{ki}}(t_{i1k}), \dots, \eta_{\sigma_{ki}}(t_{in_{ik}k}))^\top$ and $\boldsymbol{\eta}_\mu = (\boldsymbol{\eta}_{\mu_1}^\top, \dots, \boldsymbol{\eta}_{\mu_K}^\top)^\top$, $\boldsymbol{\eta}_{\mu_k} = (\boldsymbol{\eta}_{\mu_{k1}}^\top, \dots, \boldsymbol{\eta}_{\mu_{kn}}^\top)^\top$, $\boldsymbol{\eta}_{\mu_{ki}} = (\eta_{\mu_{ki}}(t_{i1k}), \dots, \eta_{\mu_{ki}}(t_{in_{ik}k}))^\top$, and diagonal matrix $\mathbf{R} = \text{diag}(\exp(\boldsymbol{\eta}_\sigma)^2)$.

3.5 Posterior mean estimation

The posterior of the full parameter vector $\boldsymbol{\theta}$ factorizes to

$$p(\boldsymbol{\theta} | \mathbf{T}, \boldsymbol{\delta}, \mathbf{y}) \propto L^{surv}(\boldsymbol{\theta} | \mathbf{T}, \boldsymbol{\delta}) \cdot L^{long}(\boldsymbol{\theta} | \mathbf{y}) \cdot \prod_{l \in \mathcal{L}} \prod_{h=1}^{\tilde{H}_l} (p(\beta_{lh} | \tau_{lh}^2) p(\tau_{lh}^2)) \cdot \prod_{m=1}^M (p(\boldsymbol{\rho}_{(m)} | \tau_{(m)}^2) p(\tau_{(m)}^2)),$$

where $\tilde{H}_l = H_l - 1$ for the longitudinal outcomes $l \in \{\mu_1, \dots, \mu_K\}$ and $\tilde{H}_l = H_l$ otherwise. We obtain starting values for the derivative-based MCMC algorithm by approximating the mode of the posterior using a blockwise Newton-Raphson procedure.[19] In contrast to Köhler et al. (2017), however, we use the approximate mode only as a starting value for mean estimation, thus prioritizing the fast convergence of the Newton-Raphson algorithm. The step length is set to 1 except for the survival predictors $l \in \{\lambda, \gamma\}$, where it is set to 0.1, and the variance parameters are initialized by the **bamlss** algorithm so that the empirical degrees of freedom are comparable across model terms.[49, 50]

Then, the MCMC algorithm uses the blockwise score vectors $\mathbf{s}(\boldsymbol{\beta}_{lh})$ and Hessian $\mathcal{H}(\boldsymbol{\beta}_{lh})$ of the log-posterior given in Appendix A to approximate the full conditionals $p(\boldsymbol{\beta}_{lh} \mid \cdot)$. [48] These approximations are based on a second-order Taylor expansion of the log-posterior centered at the last state $\boldsymbol{\beta}_{lh}^{[u]}$ for MCMC iteration u and result in a proposal density proportional to a multivariate normal distribution $N(\boldsymbol{\mu}_{lh}^{[u]}, \boldsymbol{\Sigma}_{lh}^{[u]})$ with mean $\boldsymbol{\mu}_{lh}^{[u]} = \boldsymbol{\beta}_{lh}^{[u]} - \mathcal{H}(\boldsymbol{\beta}_{lh}^{[u]})^{-1} \mathbf{s}(\boldsymbol{\beta}_{lh}^{[u]})$ and precision matrix $(\boldsymbol{\Sigma}_{lh}^{[u]})^{-1} = -\mathcal{H}(\boldsymbol{\beta}_{lh}^{[u]})$. While the calculation of the derivatives increases computational cost, it has the advantage that this MCMC algorithm approximates a Gibbs sampler, resulting in high acceptance rates and good mixing. Gibbs sampling is used for variance parameters τ_{lh}^2 with conjugate inverse Gamma hyperpriors and slice sampling otherwise.

3.6 Implementation

The implementation of the proposed approach builds on the flexibility provided by the R package **bamlss**[49, 50]. We supply the package **MJMbamlss** on Github (<https://github.com/alexvolkmann/MJMbamlss>) containing a new family-class for the presented MJM as well as some convenience functions for estimating the MFPC basis. The contained vignettes illustrate how to combine the two packages for model estimation. Similar to the package **JMbayes2**[42] we find that standardizing the survival design matrices within the estimation process improves mixing and convergence of the MCMC algorithm as well as posterior mode estimation, and is implemented by default. The integrals in the cumulative hazard rates $\Lambda_i(T_i)$ and in the corresponding derivatives are of non-standard form and we use seven point Gaussian quadrature to numerically approximate them.[37]

4 Simulations

We show the good performance of our proposed approach in two simulation scenarios. Scenario I aims at comparing our approach to the **JMbayes2**[42] package in a parametric setting that is favorable to **JMbayes2**, i.e. in a setting with a simple random intercept – random slope covariance structure, here for six longitudinal outcomes. Our approach, estimating the random effects structure nonparametrically, should be able to also recover this truly linear structure, even though a higher variance compared to correctly specifying the parametric model in **JMbayes2** is to be expected due to the increased model flexibility. This example also illustrates the reduction of parameters to estimate in our MFPC based representation, while keeping a comparable estimation performance. Scenario II by contrast focuses on a complex covariance structure, here between two nonlinear longitudinal markers, and highlights the powerful and parsimonious modeling possibilities of MFPCs for highly flexible longitudinal trajectories. In the following, the data generating processes of the two simulation scenarios are described, the general setup of the simulation is introduced, and the results are presented. Full details of the data generation, such as the used parameter values, as well as additional results are provided in Appendix B.

4.1 Scenario I

We generate a sequence of six different longitudinal trajectories for $n = 150$ subjects at an equidistant grid of 101 time points $\mathcal{P} \in [0, 1]$. The longitudinal trajectories follow a linear predictor with a fixed linear time trend and linear effect of a binary covariate x_{gi} , sampled from a discrete uniform distribution, as well as a random intercept and random slope over time. The fixed effects are chosen identical over the different longitudinal outcomes, but the random effects differ considerably in magnitude. We draw the random effects from a 12-dimensional multivariate normal distribution with mean zero and given unstructured covariance matrix. While the correlation between random intercept and slope within a longitudinal outcome is the same for all outcomes, the scale of the variances and thus covariances increases with k . At the same time, the correlation between outcomes k and l is specified as a decreasing function of their difference, i.e. “neighbouring” outcomes have a higher correlation, and equal to zero for the furthest pairs (12 of the 78 covariance parameters are zero, corresponding to independence of random effects). We specify the linear predictors η_γ as containing the binary covariate x_{gi} , the baseline hazard η_λ as following a Weibull distribution, and $\eta_{\alpha_1}, \dots, \eta_{\alpha_6}$ as constants with decreasing values from 1.5 to -1.5 . The survival times are then generated by calculating the hazard rate and deriving the corresponding survival probabilities.[3, 6] Random censoring is introduced by drawing censoring times from a uniform distribution on $[0, 1.75]$. The subject specific follow-up time T_i is the minimum of the

survival time, the censoring time and 1. We introduce subject and outcome specific observation times by sampling 25% of the remaining subject specific subset of \mathcal{P} with a maximum of 15 longitudinal observations per outcome. The longitudinal observations are then generated by adding the Gaussian noise ϵ_{ijk} with variance constant across k to the linear predictor evaluated at the observation times. In the generated data sets, all subjects have baseline measurements of the longitudinal outcomes at time point 0 so that the subjects have a minimum of six (one per outcome) and up to 90 (mean 63) longitudinal observations across all outcomes. The data sets show a mean event rate of 43%, with mean follow-up time of 0.52.

4.2 Scenario II

For simulation scenario II, we follow the same data generation structure to obtain data sets with $n = 300$ subjects and two longitudinal outcomes based on different coefficient specifications for the additive predictors compared to scenario I and a random censoring uniform distribution on $[0, 3]$. Most notably, the random intercept and slope components in the longitudinal additive predictors are replaced by a more complex covariance structure. We include multivariate functional random effects drawn from a multivariate Gaussian process with a covariance kernel based on six multivariate eigenfunctions. To do this, we follow the results for finite KL decompositions of Happ and Greven (2018)[14], and define univariate non-orthogonal basis functions and a covariance matrix for the coefficients of the corresponding basis expansion to construct the multivariate covariance kernel. We specify three basis functions per longitudinal outcome as splines with distinct characteristics at the beginning, middle, or end of the interval $[0, 1]$: For outcome 1 the basis functions correspond to level shifts, whereas for outcome 2 the basis functions describe short-term peaks (see Appendix B Figure 3). The 6×6 covariance matrix of the basis coefficients is generated from an eigenvalue decomposition with specified eigenvalues and a random orthonormal matrix. This gives a non-standard multivariate covariance kernel with highly nonlinear eigenfunctions (see Appendix B Figure 4). To generate multivariate functional random effects from this Gaussian process, we draw i.i.d. samples $\boldsymbol{\rho}_i = (\rho_{i1}, \dots, \rho_{i6})^\top \sim N_6(\mathbf{0}, \text{diag}(\nu_1, \dots, \nu_6)), i = 1, \dots, 300$ with corresponding multivariate eigenvalues ν_1, \dots, ν_6 . The data sets in scenario II have on average 24 longitudinal observations (minimum 2 and maximum 30) and a mean event rate of 57% with mean follow-up time 0.6.

4.3 Simulation Setup

For both scenarios we simulate 200 data sets to which we apply four different model estimation approaches. First, we estimate a model using the true underlying covariance kernel via the corresponding true MFPC basis in the **bamlss** framework to have an oracle benchmark model (denoted as *TRUE*). Comparing the benchmark to a model where the covariance structure is estimated from the data as described in Section 3.1 (*EST*) allows us to quantify the loss in estimation accuracy due to the MFPC basis estimation. We also visualize the impact of further reducing the number of included MFPC based random effects by lowering the truncation order M to at least 99% explained variance of the Gaussian process in a third modeling approach (*TRUNC*). Finally, we compare our proposed models to an appropriate model fit (depending on the scenario) in the widely used **JMbayes2** package (denoted as *JMB*), which also uses Bayesian model estimation with priors chosen based on preliminary separate univariate model fits for the longitudinal and survival outcomes.[42] In particular, we incorporate the knowledge of truly linear random effects and specify a random intercept – random slope model with unstructured covariance matrix for the *JMB* model in scenario I. In scenario II, the covariance structure is modeled by including a subject and outcome specific random intercept as well as three cubic B-spline basis functions resulting in an 8×8 unstructured covariance matrix. We acknowledge that this modeling approach might not be flexible enough for the specified covariance structure of the data generating process. However, increasing the number of basis functions to four already leads to numerical problems in more than 75% of the **JMbayes2** simulation runs, whereas with the proposed number only one model cannot be estimated in **JMbayes2**. Note that the **bamlss** models do not show any numerical problems in our simulation. In both frameworks, the baseline hazard is modeled using cubic P-splines with third order difference penalty and 20 basis functions (before centering).

We run the MCMC algorithm for each model for 5500 iterations and use a burnin of 500 samples and a thinning of 5 to obtain a total of 1000 samples per model. The model fits are evaluated using bias, root mean squared error (rMSE), and frequentist coverage of the 95% credible intervals of the additive predictors. In particular, we define the average bias for the longitudinal predictors $l \in \{\mu_k, \sigma_k | k = 1, \dots, K\}$ in simulation run $u = 1, \dots, 200$ as $Bias_l^u = \frac{1}{N_k^u} \sum_{i=1}^n \sum_{j=1}^{n_{ik}^u} (\hat{\eta}_{li}^u(t_{ijk}^u) - \eta_{li}^u(t_{ijk}^u))$, with estimate $\hat{\eta}_{li}^u$ and the superscript u denoting simulation run specific analogues. We also evaluate the model fit over time using a time dependent bias defined as $Bias_l^u(t) = \frac{1}{n_{risk}^u(t)} \sum_{i \in \mathcal{R}^u(t)} (\hat{\eta}_{li}^u(t) - \eta_{li}^u(t))$ for all t in \mathcal{P} , where $n_{risk}^u(t)$ is the cardinality of the risk set of subjects $\mathcal{R}^u(t)$ at time t . Note that for the survival submodel, we evaluate the survival predictors η_λ and η_γ jointly using their sum $\eta_{\lambda+\gamma}$, as the two frameworks handle intercepts and sum-to-zero constraints for smooth effects differently. For $l \in \{\lambda + \gamma, \alpha_1, \dots, \alpha_K\}$ we calculate the average bias $Bias_l^u = \frac{1}{n} \sum_{i=1}^n (\eta_{li}^u(T_i^u) - \hat{\eta}_{li}^u(T_i^u))$

Table 1: Results of simulation scenario I. The bias and rMSE values for $\eta_{\mu_1}, \dots, \eta_{\mu_6}$ are multiplied by factor 100 for better readability. The values for $\eta_{\sigma_1}, \dots, \eta_{\sigma_6}$ are averaged and reported as η_{σ} .

η	Bias				rMSE				Coverage			
	<i>TRUE</i>	<i>EST</i>	<i>TRUNC</i>	<i>JMB</i>	<i>TRUE</i>	<i>EST</i>	<i>TRUNC</i>	<i>JMB</i>	<i>TRUE</i>	<i>EST</i>	<i>TRUNC</i>	<i>JMB</i>
$\lambda + \gamma$	0.811	0.812	0.812	1.006	0.907	0.911	0.909	1.124	0.438	0.433	0.436	0.465
α_1	0.118	0.106	0.126	0.042	0.313	0.315	0.338	0.283	0.945	0.930	0.920	0.955
α_2	0.014	0.014	0.012	0.003	0.256	0.261	0.267	0.242	0.950	0.955	0.965	0.970
α_3	0.047	0.035	0.029	0.006	0.214	0.211	0.220	0.199	0.955	0.970	0.965	0.965
α_4	-0.053	-0.046	-0.052	-0.046	0.208	0.213	0.216	0.198	0.945	0.945	0.935	0.955
α_5	-0.061	-0.056	-0.054	-0.051	0.201	0.199	0.199	0.186	0.965	0.955	0.955	0.970
α_6	-0.168	-0.157	-0.158	-0.106	0.259	0.251	0.256	0.227	0.905	0.895	0.905	0.960
μ_1	0.003	0.004	0.003	0.004	2.510	4.785	9.786	2.516	0.949	0.843	0.673	0.948
μ_2	0.001	0.000	-0.000	-0.004	2.516	4.872	9.005	2.522	0.948	0.842	0.715	0.946
μ_3	-0.004	-0.003	-0.003	-0.010	2.507	5.079	8.250	2.511	0.950	0.839	0.755	0.947
μ_4	0.004	0.004	0.004	0.002	2.523	5.363	6.944	2.528	0.949	0.834	0.796	0.947
μ_5	-0.002	-0.002	-0.002	-0.003	2.518	5.463	6.377	2.522	0.950	0.831	0.807	0.949
μ_6	0.011	0.012	0.011	0.011	2.527	5.914	6.240	2.531	0.950	0.827	0.817	0.948
σ	0.002	0.263	0.467	0.001	0.016	0.263	0.467	0.016	0.945	0.056	0.028	0.938

at the subject specific follow-up times as well as the time dependent bias $Bias_l^u(t)$ as above. We define the rMSE and the coverage analogously for all predictors, for instance $rMSE_l^u = (\frac{1}{n} \sum_{i=1}^n (\hat{\eta}_i^u(T_i^u) - \eta_i^u(T_i^u))^2)^{1/2}$ and $Coverage_l^u = \frac{1}{n} \sum_{i=1}^n I(\hat{\eta}_i^{u,2.5}(T_i^u) \leq \eta_i^u(T_i^u) \leq \hat{\eta}_i^{u,97.5}(T_i^u))$ with indicator function $I(\cdot)$ and $\hat{\eta}^{u,\alpha}$ the $\alpha\%$ quantile of the MCMC samples for the posterior mean for the survival predictors $l \in \{\lambda + \gamma, \alpha_1, \dots, \alpha_K\}$. Naturally, these definitions simplify correspondingly for the predictors $l \in \{\alpha_1, \dots, \alpha_K, \sigma_1, \dots, \sigma_K\}$, which are constant over all subjects and time in our simulation. The evaluation criteria of the 200 (or 199 for the **JMbayes2** approach in scenario II) simulation runs are then averaged for presentation.

Additionally, we evaluate the estimated MFPCs in both scenarios. Eigenfunctions are generally only defined up to a sign change, which is why we first use the norm $\|\cdot\|$ induced by (5) (with weights chosen as 1 throughout the simulation) to determine whether a reflected version $(-\hat{\psi}_m(t))$ is closer to the true eigenfunction $\psi_m(t), m = 1, \dots, M$. We then use the squared norm of the error, $\|\psi_m - \hat{\psi}_m\|^2$, to evaluate the estimated MFPC.

4.4 Simulation results

Table 1 contains the results of simulation scenario I. Comparing the **bamlss** model *TRUE* with true underlying eigenfunctions as basis functions to the **JMbayes2** model *JMB* allows to directly compare the two frameworks for MJMs, contrasting the different choices of basis and correlation structure without influence of the particular method used to estimate the MFPCs. More precisely, while both approaches predict the two random effects for each subject in their model fit, the MFPC based approach only estimates the random effect variances whereas **JMbayes2** also estimates the correlation between the random intercepts and slopes on all longitudinal outcomes. Overall, we find that the two approaches yield similar bias and rMSE values in the linear scenario I. In more detail, **bamlss** performs slightly better for the survival predictors $\eta_{\lambda} + \eta_{\gamma}$ and the longitudinal predictors $\eta_{\mu_1}, \dots, \eta_{\mu_6}$, while the **JMbayes2** approach results in better estimates of the association predictors $\eta_{\alpha_1}, \dots, \eta_{\alpha_6}$. Aside from the different prior specifications, some of this difference in performance for the η_{α_k} might also be caused by the relatively short MCMC chains to lower the computational burden of the simulation. The frequentist coverage of both frameworks is close to the nominal value of 95% for all predictors except the combined survival predictor containing the baseline hazard. Bender et al. (2018)[2] point out that using P-splines with a single penalty/variance parameter can be suboptimal when the baseline hazard changes quickly over the follow-up period and suggest to use adaptive spline smooths instead, which is only available (at increased computational cost) for **bamlss** and not for **JMbayes2**, and thus not used in this comparison.

Estimating the MFPC basis functions from the data results in a clear increase in the variance of the estimated longitudinal submodel, due to the higher flexibility of our nonparametric approach, which gives an advantage to the correctly specified parametric *JMB* and *TRUE* models (the latter using the true linear MFPCs). The higher variability is reflected in higher rMSE values of the *EST* models, while the bias values for the longitudinal predictors remain stable. The reason is that flexibly estimating the eigenfunctions from the data in scenario I does not necessarily result in linear estimated MFPCs (see Appendix B Figure 6), which can lead to longitudinal model fits that are too wiggly compared to the true parametric random intercept – random slope data generating process assumed known in *JMB* and *TRUE* models. This mixing of the correlation structure and the random noise also leads to an overestimation of the variance predictors $\eta_{\sigma_1}, \dots, \eta_{\sigma_6}$ (averaged in Table 1) coupled with poor frequentist coverage in the longitudinal submodel. This, however, does not negatively affect the estimation of the survival submodel where the bias, rMSE, and coverage values are similar to the *TRUE* models, including for the association predictors $\eta_{\alpha_1}, \dots, \eta_{\alpha_6}$. Note that the bias and rMSE values for the longitudinal predictors in Table 1 have been multiplied by a factor 100, such that the longitudinal model fits using the estimated MFPCs

Table 2: Results of simulation scenario II. The bias and rMSE values for $\eta_{\mu_1}, \eta_{\mu_2}$ are multiplied by factor 100 for better readability.

η	Bias				rMSE				Coverage			
	<i>TRUE</i>	<i>EST</i>	<i>TRUNC</i>	<i>JMB</i>	<i>TRUE</i>	<i>EST</i>	<i>TRUNC</i>	<i>JMB</i>	<i>TRUE</i>	<i>EST</i>	<i>TRUNC</i>	<i>JMB</i>
$\lambda + \gamma$	1.087	1.129	1.135	1.473	1.185	1.223	1.228	1.545	0.154	0.147	0.148	0.103
α_1	0.019	0.012	0.012	-0.053	0.070	0.072	0.073	0.098	0.945	0.935	0.950	0.849
α_2	0.010	0.005	0.002	-0.043	0.070	0.074	0.079	0.104	0.990	0.960	0.955	0.859
μ_1	-0.004	-0.004	-0.006	-0.002	2.894	11.271	12.808	13.013	0.944	0.795	0.770	0.810
μ_2	-0.027	-0.028	-0.027	-0.036	2.850	8.917	9.752	20.246	0.934	0.783	0.776	0.791
σ_1	0.021	0.805	0.894	0.955	0.027	0.805	0.894	0.955	0.835	0.000	0.000	0.000
σ_2	0.019	0.625	0.662	1.364	0.023	0.625	0.662	1.364	0.790	0.000	0.000	0.000

still are visually close to the true trajectories (see Appendix B Figure 5) and seem close enough to correctly estimate the association predictors well.

Lowering the number of MFPC basis functions included in the model by introducing truncation at a pre-specified rate of explained variance of the Gaussian process is expected to lower the computational burden, but to deteriorate the longitudinal submodel fit. In particular, for a truncation at 99% explained variance, the *TRUNC* models offer a notable dimension reduction, as most models only include ten MFPCs (minimum nine and maximum eleven) instead of the full 12, thus cutting down the models by 2×150 parameters. While the bias values of the longitudinal predictors are basically unaffected by the truncation, we note that the rMSE values of the longitudinal predictors are up to four times higher while the frequentist coverage drops to about 70–80%. The variation of the Gaussian process now unaccounted for by the excluded MFPCs is absorbed by the variance predictors $\eta_{\sigma_1}, \dots, \eta_{\sigma_6}$, which are overestimated throughout all *TRUNC* models. The *TRUNC* models show, however, that the trailing MFPCs with small variances mainly affect the fit of the longitudinal submodel (see Appendix B Figure 5) while the association predictors are still estimated reasonably well. Truncation thus allows an explicit choice and trade-off between computational complexity and (longitudinal) model fit, with the ordering of eigenvalues ensuring that components of little importance are truncated first.

In simulation scenario II, the parametric covariance specification of scenario I is replaced by a complex multivariate covariance structure. In this setting, the *JMB* models based on the **JMbayes2** framework no longer have the advantage of “knowing” the correct parametric model. In fact, we find that the restricted flexibility of the *JMB* models (as mentioned above) leads to a worse overall model fit compared to *TRUE* models as measured by the bias, rMSE, and frequentist coverage values for (almost) all predictors as given in Table 2. The difference between the two models is especially pronounced for the longitudinal predictors $\eta_{\mu_1}, \eta_{\mu_2}$, and $\eta_{\sigma_1}, \eta_{\sigma_2}$, but also for the association predictors $\eta_{\alpha_1}, \eta_{\alpha_2}$. A negative bias for positive values of the underlying association in simulation II indicates that the *JMB* models underestimate the association parameters. Figure 1 illustrates for three random subjects that the *TRUE* model using the underlying eigenfunctions as basis functions fits closely to the true trajectories, while the *JMB* model tends to oversmooth the data, which may explain its slight underestimation of the α_1, α_2 association parameters also known to occur in regression settings with covariate measurement error[4]. Especially for subjects with a short follow-up time (such as subject 56), principal component based random effects may be more capable of pooling the information over all subjects and across markers to approximate the true trajectories, while in the example of subject 56 in Figure 1 the *JMB* model even fits an incorrectly increasing time trend based on the few data points available.

Similar to scenario I, the estimation of the MFPC basis mainly increases the variance of the estimates in the longitudinal submodel, with rMSE values still lower than in the **JMbayes2** framework. The corresponding coverage drops to about 80% for the longitudinal predictors and the variance predictors are overestimated with a coverage of 0, both similar to the *JMB* model. Figure 1 exemplifies that the longitudinal submodel fits are still sufficiently close to the true trajectories for the estimation of the association predictors $\eta_{\alpha_1}, \eta_{\alpha_2}$ not to suffer from the estimation of the MFPC basis. Truncating the basis to 99% of explained variance again entails a slight deterioration in the overall model fit as reported by the bias, rMSE, and coverage. Note, however, that in 64% of all simulation runs all six MFPCs are included in the *TRUNC* models. Further decreasing the truncation threshold to 95% (results not shown) lowers the computational burden by reducing the number of MFPC basis functions from six to on average four, thus dropping 2×300 parameters. The resulting decline in estimation accuracy, however, is so considerable that the rMSE values are then higher than for the oversmoothed *JMB* models for both the longitudinal and the association predictors. We conclude that truncation needs to be carefully considered and that a large percentage of variation should be retained unless prohibited by computational considerations.

The time dependent evaluation in both simulation scenarios (results not shown) reveals that the estimation of the baseline hazard with P-splines in both frameworks leads to oversmoothing at the beginning of the time interval, where the baseline hazard is quickly changing (cf. Bender et al., 2018[2]), explaining results in the first rows of Tables 1 and 2. For the longitudinal submodel, the drop-out process implies less information at

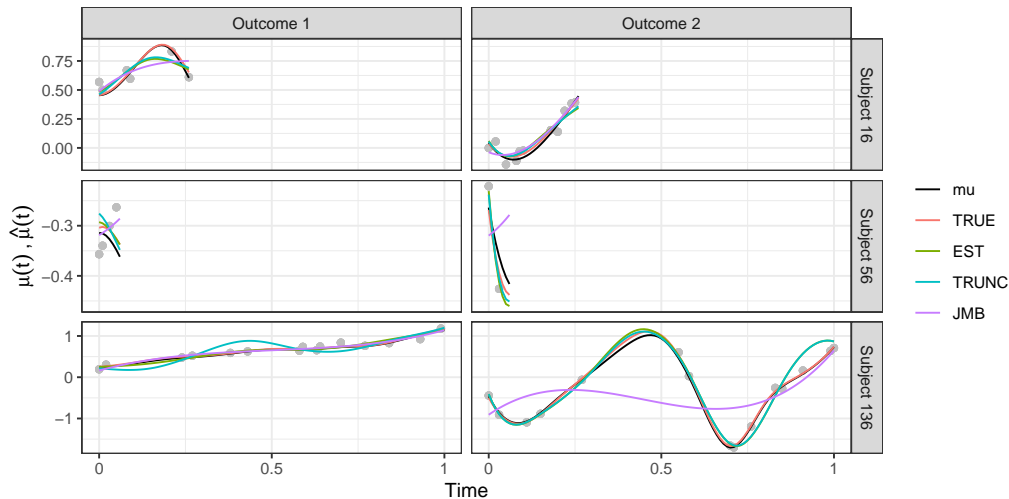


Figure 1: Different model fits of the longitudinal submodel for three random subjects of a simulated data set in scenario II. The solid black line corresponds to the true underlying longitudinal trajectory (μ) and the grey dots are the observed data points. The *TRUNC* model in this example includes five MFPCs instead of the correct six.

the end of the time interval, resulting in decreasing estimation accuracy. As the drop-out process also affects the estimation of the MFPC basis functions and as this additional uncertainty is not reflected in the *EST* and *TRUNC* models, this also results in decreasing coverage over time.

The results from both simulation scenarios reinforce that the choice and for MFPCs also estimation of the basis is an essential prerequisite for a satisfactory model fit. We see in scenario I that if the covariance structure is known to be parametric a priori, a parametric model will always perform better than our more flexible nonparametric specification, which by estimating the linear eigenfunctions introduces additional noise into the MFPCs. On the other hand, parametric or less flexible spline specifications are not sufficient to capture more complex trends and result in oversmoothing, such as in scenario II, where our more flexible approach has a clear advantage. We find that estimated MFPCs (see Appendix B Figure 7) in most simulation runs recover the relevant characteristics of the eigenfunctions and thus time trends well, with the leading MFPCs closer to the true eigenfunctions in simulation scenario II (cf. Table 4 in the Appendix). This illustrates again that the strength of our proposed MFPC based approach lies in the estimation of complex covariance structures. For both simulation scenarios, we find that lowering the truncation threshold can considerably decrease the estimation accuracy of the longitudinal submodel and even negatively affect the survival submodel. We therefore advocate to use a high rate of explained variance, such as 99%, for determining the number of MFPCs in a model.

5 Application

We demonstrate our parsimonious but flexible modeling approach by analyzing a PBC study, where we want to model the association between different biochemical markers and the survival of the patients, and compare it to the more parameter intensive modeling approach of using spline based random effects to capture the (potentially) complex covariance structure in the data. The code to reproduce the analysis is provided in the accompanying R package **MJMbamls**. The PBC data provided in the R package **JMbayes2** include information on 312 subjects, in particular on the follow-up time (composite event of liver transplantation or death), baseline covariates (sex, age, and treatment group), and several longitudinally measured biochemical outcomes which are suspected to be associated with disease progression. During the study period, visits were scheduled but missing observations and drop out lead to irregular measurements of the longitudinal outcomes with an average of 6.2 visits per subject. At the end of the study period, 169 subjects had experienced the event with median follow-up time of 4.5 years (IQR: 2.2, 6.5) and 143 subjects were event-free with median follow-up time of 8.7 (IQR: 6.5, 10.5). For our analysis, we include the continuous longitudinal outcomes *albumin* in g/dl, serum bilirubin (*serBilir*) in mg/dl, serum cholesterol (*serChol*) in mg/dl, and aspartate aminotransferase (*SGOT*) in U/liter, all log-transformed to improve adherence to the normal assumption.[34] For a more direct comparison to the **JMbayes2** framework, eight subjects for whom no measurements of serum cholesterol are available are excluded from the analysis, giving a total of 304 subjects. We use all available baseline information on the subjects such as *age* at registration in years, *sex* (male or female), and treatment group *drug* (placebo or D-penicillamine) for modeling the hazard as well as the longitudinal outcomes. Note that we cap the follow-up

times t at the maximum observation time of longitudinal measurements in the data set (14.1 years, only affecting three event-free subjects) to avoid extrapolation of the longitudinal trajectories.

We apply the proposed MFPC based approach (denoted as *bamlss*) to the PBC data and compare the results to a similarly specified model fit of the **JMbayes2** package (denoted as *JMB*). These models follow the specifications (1) – (4) with

$$\begin{aligned}\eta_{\gamma i} &= \beta_{\gamma 0} + \beta_{\gamma 1} \cdot \text{sex}_i + \beta_{\gamma 2} \cdot \text{drug}_i + f_{\gamma}(\text{age}_i), \\ \eta_{\alpha_k i}(t) &= \beta_{\alpha_k}, \\ \eta_{\mu_k i}(t) &= \beta_{k0} + \beta_{k1} \cdot \text{sex}_i + \beta_{k2} \cdot \text{drug}_i + f_{k1}(\text{age}_i) + f_{k2}(t) + b_i^{(k)}(t), \text{ and} \\ \eta_{\sigma_k i}(t) &= \beta_{\sigma_k}\end{aligned}$$

for $k \in \{\text{albumin}, \text{serBilir}, \text{serChol}, \text{SGOT}\}$, and subject index i . To include a smooth time trend for the longitudinal outcomes and to allow for possibly nonlinear covariate effects of age, we use P-splines with ten basis functions before centering to estimate the additive functions f_{γ} , f_{k1} , and f_{k2} with **bamlss**. For the **JMbayes2** model we try to fully exploit the framework’s flexibility but for a natural cubic B-spline basis, we reach the limit with three basis functions, as more basis functions result in error messages. Similarly, we use the MFPC based representation (6) to estimate the longitudinal random effects in our approach, while the **JMbayes2** model maximally allows random intercepts and a natural cubic splines representation of the follow-up time with two basis functions, giving three random effects per subject and longitudinal outcome. The baseline hazard $\eta_{\lambda i}(t)$ is modeled in both frameworks using cubic P-splines with second order difference penalty and 10 basis functions (before centering).

For the estimation of the MFPC basis, we follow the outline given in section 3.1. In order to obtain stable estimates of univariate scores, the UFPCAs are based on a subset of 145 subjects that have at least three longitudinal measurements and one measurement after 10% of the follow-up time interval. We use seven marginal B-spline basis functions for the estimation of the univariate covariance functions and truncate the UFPCA at 99% explained univariate variance, which results in three UFPCs per longitudinal outcome. The resulting eigenvalues of the UFPCAs show a considerable imbalance in univariate variation in the data with marker *serBilir* exhibiting an integrated univariate variance more than 70 times larger than that of *albumin*. By using a scalar product (5) with weights inversely proportional to the integrated univariate variance for the MFPCA, we account for the different amounts of variation equivalent to standardizing the longitudinal data without actually transforming the outcome. The resulting MFPCs are then more balanced across the longitudinal outcomes with the first two explaining 51.2% and 22.8% of the weighted variance, respectively, while using scalar product weights of 1 would give a first MFPC dominated by *serBilir* accounting for 79.5% of the (unweighted) multivariate variance. In a sensitivity analysis (see Appendix C) we use the estimated MFPCs of the unweighted MFPCA and find that the model fits better to the *serBilir* data but worse to the other markers giving an overall worse model fit. Visual inspection of the estimated MFPCs (see Appendix C Figure 8) shows that using seven B-spline basis functions in the univariate specifications yields a good compromise between overly smooth and too flexible (trailing) MFPCs. To decrease the computational burden of the final model fit, we truncate the MFPC basis at 99% explained variance, which leads to nine included MFPCs for the weighted MFPCA models, i.e. roughly a parsimonious two basis functions per marker.

For each model, we run one MCMC chain with 12,000 iterations, a burnin of 2,000 and a thinning of 5, yielding 2,000 samples. Overall, we find that the MFPC based *bamlss* model yields similar results to the spline based random effects approach of the *JMB* model. In particular, Table 3 shows that we find significant association of the time-to-event process with the current value of each biochemical marker of our analysis, irrespective of the modeling approach used. This finding aligns with other works in the literature[1, 44, 47], who might have come to slightly different conclusions due to different model specifications. Other estimated parameters such as the linear effects of *sex* on the hazard or the longitudinal outcomes are also similar for the *bamlss* and *JMB* models (see Appendix C Table 5). What is more, Figure 2 illustrates that the longitudinal submodel fits of both models are generally very close. Given that the estimated MFPC basis could provide much more flexibility than the spline approach with only two basis functions, this suggests that the PBC data might not require the added flexibility supplied by an MFPC basis representation. Nevertheless, the *bamlss* model uses much fewer parameters for the estimation of the random effects structure despite the larger flexibility. While the spline based approach estimates $3 \times 4 \times 304$ random effects with an unstructured covariance matrix of 78 covariance parameters, the MFPC based approach only needs 9×304 random effects with a diagonal covariance matrix of 9 variance parameters, thus saving $3 \times 304 + 69 = 981$ parameters total. We therefore show that using an MFPC basis not only reduces the computational costs of fitting an MJM, but also constitutes an alternative, highly flexible modelling approach to spline based random effects, especially when numerical problems restrict their usage for nonlinear covariance structures. Then the proposed approach also allows to check whether the assumptions made in a spline model with few basis functions dictated by computational possibilities are in fact warranted.

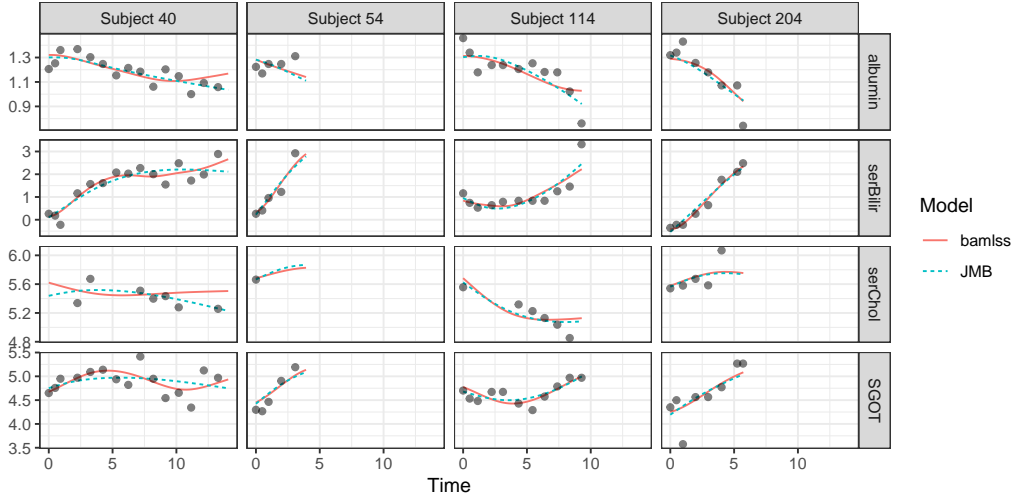


Figure 2: MFPC based (*bamlss*) and spline based (*JMB*) model fits of the PBC data for four subjects. The grey dots are the observed data points. Longitudinal outcomes are log-transformed.

Table 3: Posterior mean and 95% credible interval of the association predictors β_{α_k} for the two models also shown in Figure 2. Longitudinal outcomes are log-transformed.

	<i>bamlss</i>		<i>JMB</i>	
<i>albumin</i>	-5.82	[-7.84; -3.89]	-6.03	[-7.87; -4.24]
<i>serBilir</i>	1.48	[1.19; 1.77]	1.39	[1.11; 1.68]
<i>serChol</i>	-0.76	[-1.36; -0.16]	-0.68	[-1.26; -0.06]
<i>SGOT</i>	-0.74	[-1.41; -0.13]	-0.76	[-1.4; -0.11]

6 Discussion and Outlook

We have shown that shared parameter MJMs can greatly benefit from using an MFPC based representation of the random effects structure. In particular, the flexibility when modeling highly nonlinear subject specific trends in the multivariate longitudinal outcomes is often restricted by the computational complexity of the number of parameters to estimate, especially when a spline approach is used. Using MFPCs as a basis for random effects allows a parsimonious representation of increased flexibility, reducing the number of parameters to estimate by decoupling it from the number of longitudinal outcomes and simplifying the covariance structure of the random effects. Our simulation study showcases that the MFPC based approach can achieve a better model fit for nonlinear longitudinal outcome trajectories resulting also in a more accurate estimation of the association structure with the event hazard. Furthermore, the explicit ordering of the MFPCs in terms of explained variance makes the trade-off between computational burden and goodness of fit explicit, which allows its steering by the selection of the truncation level for the number of MFPC based random effects. Note that while not focused on here, dynamic prediction for subjects with incoming new longitudinal measurements is directly available from our approach since the estimated MFPCs are used as empirical basis functions also for all (new) subjects in the proposed MJM, and the standard algorithms for dynamic prediction of the random scores can thus be used.[41]

We also provide a working implementation for the framework of flexible MJMs in the **bamlss** package, which supports a vast range of possible specifications for covariate effects in a user friendly way. Note, however, that the idea of an MFPC basis is more universal and can be combined with different approaches to shared parameter MJMs such as approximations using adapted two-stage models[28] or integrated nested Laplace (INL)[44]. For **JMbayes2**, both the simulation study and our application have shown that the model flexibility is restricted by the number of spline basis functions which can be included in the longitudinal submodel. This could be mitigated by implementing our proposed MFPC approach also in **JMbayes2**. Additionally, Rustand et al. (2020)[44] remark that simplifying the random effects covariance matrix to be block-diagonal considerably reduces computation times. While this corresponds to the strong assumption of independent random effects across markers, an MFPC basis does in fact provide the further simplification of a diagonal covariance matrix without the necessity of such an independence assumption. On the other hand, both the adapted two-stage and the INL approximations to the full MJM present computational advantages to the derivative based MCMC sampling implemented in **bamlss**. In simulation scenario I, for example, the fully Bayesian approach in **bamlss** estimates the MJM in around 30 minutes on a Linux system with 12 cores at 3.5 GHz and 32 GB memory while

the highly optimized approach in **JMbayes2** returns results after roughly one minute with the same setup. This difference might in future be diminished by increasing computational efficiency in the implemented code via transferring more computations to other languages such as C or exploiting sparse structures in the design matrices. A combination of an MFPC approach and approximate approaches also holds promise.

It is important to note, however, that estimating the MFPC basis is an integral part of our proposed model estimation approach. Besides model selection criteria such as the Bayesian information criterion or the deviance information criterion, we find that examination of the amount of variance explained and visual inspection of the estimated UFPCs and MFPCs is helpful to select the number of MFPCs and assure that the fitted longitudinal trajectories in the MJM exhibit a reasonable amount of flexibility. Our current approach of estimating the MFPC basis ignores the informative missingness of the longitudinal process by treating the longitudinal outcomes as sparsely observed functional data. While we are able to show that the resulting estimated MFPCs serve as a sufficiently good empirical basis in the MJM, we encourage further research on estimating UFPCs and MFPCs under informative censoring. Several ad-hoc adjustments might improve the efficient use of all available longitudinal information such as weighting univariate outcomes depending on their length of follow-up in the estimation of the univariate covariance structure instead of excluding subjects with short follow-up time from the MFPCA entirely. Dong et al. (2023)[7] suggest that the UFPC estimation under informative censoring might be improved by iteratively estimating UFPCs and predicting the full longitudinal trajectories, as this might stabilize estimation. Alternatively, separate univariate joint models based on reduced rank models, which simultaneously estimate the time-to-event process and the UFPCs as in Yao (2007)[57], could be employed, but would considerably increase computational burden. Further research is needed to evaluate and compare different approaches to estimate UFPCs under informative missingness.

As a consequence of the proposed two step approach, all model based inference is conditional on the estimated MFPCs. Since Happ and Greven [14] show that the MFPC estimates asymptotically converge to the true eigenfunctions, the inference can be expected to be asymptotically correct. Future work is needed to account for the uncertainty in the estimation of the MFPC basis in finite samples, for example using corrections along the lines of Goldsmith et al. (2013)[11], which would improve the frequentist coverage properties of the longitudinal submodel fits. Developing an estimation approach which jointly estimates the scores and MFPCs within an MJM might further enhance modeling and understanding of the longitudinal processes, also allowing for inference regarding the estimated MFPCs.

Given that an MFPC based representation of random effects is a universal and effective approach for MJMs, future work can follow several more research avenues. From extending the presented joint model to incorporate functional covariates, functional outcomes, or different parameterizations of the association structure between the longitudinal and time-to-event submodels, to developing efficient approximations to the full derivative based MCMC algorithm in our **bamlss** implementation or advancing the MFPC basis approach to non-normal longitudinal outcomes, MJMs remain an interesting and challenging field of study.

7 Acknowledgements

We gratefully acknowledge funding by grant GR 3793/3-1 ‘Flexible regression methods for curve and shape data’ from the German Research Foundation (DFG).

References

- [1] E.-R. Andrinopoulou and D. Rizopoulos. Bayesian shrinkage approach for a joint model of longitudinal and survival outcomes assuming different association structures. *Statistics in Medicine*, 35(26):4813–4823, 2016.
- [2] A. Bender, A. Groll, and F. Scheipl. A generalized additive model approach to time-to-event analysis. *Statistical Modelling*, 18(3-4):299–321, 2018.
- [3] R. Bender, T. Augustin, and M. Blettner. Generating survival times to simulate cox proportional hazards models. *Statistics in Medicine*, 24(11):1713–1723, 2005.
- [4] R. J. Carroll, D. Ruppert, L. A. Stefanski, and C. M. Crainiceanu. *Measurement error in nonlinear models: a modern perspective*. Chapman and Hall/CRC, 2006.
- [5] J. Cederbaum, F. Scheipl, and S. Greven. Fast symmetric additive covariance smoothing. *Computational Statistics & Data Analysis*, 120:25–41, 2018.
- [6] M. J. Crowther and P. C. Lambert. Simulating biologically plausible complex survival data. *Statistics in Medicine*, 32(23):4118–4134, 2013.

- [7] J. Dong, H. Shi, L. Wang, Y. Zhang, and J. Cao. Jointly modelling multiple transplant outcomes by a competing risk model via functional principal component analysis. *Journal of Applied Statistics*, 50(1): 43–59, 2023.
- [8] C. L. Faucett and D. C. Thomas. Simultaneously modelling censored survival data and repeatedly measured covariates: a gibbs sampling approach. *Statistics in Medicine*, 15(15):1663–1685, 1996.
- [9] T. R. Fleming and D. P. Harrington. *Counting processes and survival analysis*, volume 625. John Wiley & Sons, 2013.
- [10] I. Goldschmidt, A. Karch, R. Mikolajczyk, F. Mutschler, N. Junge, E. D. Pfister, T. Möhring, L. d’Antiga, P. McKiernan, D. Kelly, et al. Immune monitoring after pediatric liver transplantation—the prospective chilfree cohort study. *BMC Gastroenterology*, 18:1–9, 2018.
- [11] J. Goldsmith, S. Greven, and C. Crainiceanu. Corrected confidence bands for functional data using principal components. *Biometrics*, 69(1):41–51, 2013.
- [12] B. Goodrich, J. Gabry, I. Ali, and S. Brilleman. **rstanarm**: Bayesian applied regression modeling via Stan. ”<https://mc-stan.org/rstanarm>”, 2020. R package version 2.21.1.
- [13] L. Hakola, M. E. Miettinen, E. Syrjälä, M. Åkerlund, H.-M. Takkinen, T. E. Korhonen, S. Ahonen, J. Ilonen, J. Toppari, R. Veijola, et al. Association of cereal, gluten, and dietary fiber intake with islet autoimmunity and type 1 diabetes. *JAMA Pediatrics*, 173(10):953–960, 2019.
- [14] C. Happ and S. Greven. Multivariate functional principal component analysis for data observed on different (dimensional) domains. *Journal of the American Statistical Association*, 113(522):649–659, 2018.
- [15] G. L. Hickey, P. Philipson, A. Jorgensen, and R. Kolamunnage-Dona. joinerml: a joint model and software package for time-to-event and multivariate longitudinal outcomes. *BMC Medical Research Methodology*, 18:1–14, 2018.
- [16] S. Holte, T. Randolph, J. Ding, J. Tien, R. McClelland, J. Baeten, and J. Overbaugh. Efficient use of longitudinal cd4 counts and viral load measures in survival analysis. *Statistics in Medicine*, 31(19): 2086–2097, 2012.
- [17] Y. Hong, L. Su, S. Song, and F. Yan. Dynamic prediction of disease processes based on recurrent history and functional principal component analysis of longitudinal biomarkers: Application for ovarian epithelial cancer. *Statistics in Medicine*, 40(8):2006–2023, 2021.
- [18] K. Kang and X. Y. Song. Joint modeling of longitudinal imaging and survival data. *Journal of Computational and Graphical Statistics*, 32(2):402–412, 2023.
- [19] M. Köhler, N. Umlauf, A. Beyerlein, C. Winkler, A.-G. Ziegler, and S. Greven. Flexible bayesian additive joint models with an application to type 1 diabetes research. *Biometrical Journal*, 59(6):1144–1165, 2017.
- [20] M. Köhler, N. Umlauf, and S. Greven. Nonlinear association structures in flexible bayesian additive joint models. *Statistics in Medicine*, 37(30):4771–4788, 2018.
- [21] D. Kong, J. G. Ibrahim, E. Lee, and H. Zhu. Flcrm: Functional linear cox regression model. *Biometrics*, 74(1):109–117, 2018.
- [22] C. Li, L. Xiao, and S. Luo. Joint model for survival and multivariate sparse functional data with application to a study of alzheimer’s disease. *Biometrics*, 78(2):435–447, 2022.
- [23] K. Li and S. Luo. Functional joint model for longitudinal and time-to-event data: an application to alzheimer’s disease. *Statistics in Medicine*, 36(22):3560–3572, 2017.
- [24] K. Li and S. Luo. Bayesian functional joint models for multivariate longitudinal and time-to-event data. *Computational Statistics & Data Analysis*, 129:14–29, 2019.
- [25] K. Li and S. Luo. Dynamic prediction of alzheimer’s disease progression using features of multiple longitudinal outcomes and time-to-event data. *Statistics in Medicine*, 38(24):4804–4818, 2019.
- [26] N. Li, Y. Liu, S. Li, R. M. Elashoff, and G. Li. A flexible joint model for multiple longitudinal biomarkers and a time-to-event outcome: With applications to dynamic prediction using highly correlated biomarkers. *Biometrical Journal*, 63(8):1575–1586, 2021.

- [27] J. Lin, K. Li, and S. Luo. Functional survival forests for multivariate longitudinal outcomes: Dynamic prediction of alzheimer’s disease progression. *Statistical Methods in Medical Research*, 30(1):99–111, 2021.
- [28] K. Mauff, E. Steyerberg, I. Kardys, E. Boersma, and D. Rizopoulos. Joint models with multiple longitudinal outcomes and a time-to-event outcome: a corrected two-stage approach. *Statistics and Computing*, 30:999–1014, 2020.
- [29] K. Mauff, N. S. Erler, I. Kardys, and D. Rizopoulos. Pairwise estimation of multivariate longitudinal outcomes in a bayesian setting with extensions to the joint model. *Statistical Modelling*, 21(1-2):115–136, 2021.
- [30] J. Murray. Package ‘gmvjoint’: Joint models of survival and multivariate longitudinal data. ”<https://github.com/jamesmurray7/gmvjoint>”, 2023.
- [31] J. Murray and P. Philipson. A fast approximate em algorithm for joint models of survival and multivariate longitudinal data. *Computational Statistics & Data Analysis*, 170:107438, 2022.
- [32] J. Murray and P. Philipson. Fast estimation for generalised multivariate joint models using an approximate em algorithm. *Computational Statistics & Data Analysis*, page 107819, 2023.
- [33] P. A. Murtaugh, E. R. Dickson, G. M. Van Dam, M. Malinchoc, P. M. Grambsch, A. L. Langworthy, and C. H. Gips. Primary biliary cirrhosis: prediction of short-term survival based on repeated patient visits. *Hepatology*, 20(1):126–134, 1994.
- [34] S. Pandolfi, F. Bartolucci, and F. Pennoni. A hidden markov model for continuous longitudinal data with missing responses and dropout. *Biometrical Journal*, page 2200016, 2023.
- [35] G. Papageorgiou, K. Mauff, A. Tomer, and D. Rizopoulos. An overview of joint modeling of time-to-event and longitudinal outcomes. *Annual Review of Statistics and Its Application*, 6:223–240, 2019.
- [36] P. Philipson, G. L. Hickey, M. J. Crowther, and R. Kolamunnage-Dona. Faster monte carlo estimation of joint models for time-to-event and multivariate longitudinal data. *Computational Statistics & Data Analysis*, 151:107010, 2020.
- [37] W. H. Press, S. A. Teukolsky, W. T. Vetterling, and B. P. Flannery. *Numerical Recipes: The Art of Scientific Computing*. Cambridge University Press, New York, 3rd edition, 2007. ISBN 9780521884075.
- [38] C. Proust-Lima and J. M. Taylor. Development and validation of a dynamic prognostic tool for prostate cancer recurrence using repeated measures of posttreatment psa: a joint modeling approach. *Biostatistics*, 10(3):535–549, 2009.
- [39] J. O. Ramsay and B. W. Silverman. *Functional data analysis*. Springer Science & Business Media, second edition, 2005.
- [40] D. Rizopoulos. *Joint models for longitudinal and time-to-event data: With applications in R*. CRC press, 2012.
- [41] D. Rizopoulos. The r package **JMbayes** for fitting joint models for longitudinal and time-to-event data using mcmc. *Journal of Statistical Software*, 72(7):1–46, 2016.
- [42] D. Rizopoulos, G. Papageorgiou, and P. Miranda Afonso. **JMbayes2**: Extended joint models for longitudinal and time-to-event data. <https://github.com/drizopoulos/JMbayes2>, 2022. <https://drizopoulos.github.io/JMbayes2/>.
- [43] D. Rizopoulos, G. Papageorgiou, and P. Miranda Afonso. **JMbayes2**: Extended joint models for longitudinal and time-to-event data. <https://CRAN.R-project.org/package=JMbayes2>, 2023. URL <https://CRAN.R-project.org/package=JMbayes2>. R package version 0.4-5.
- [44] D. Rustand, J. van Niekerk, E. T. Krainski, H. Rue, and C. Proust-Lima. Fast and flexible inference for joint models of multivariate longitudinal and survival data using integrated nested laplace approximations. *Biostatistics*, page kxad019, 2023.
- [45] F. Scheipl, A.-M. Staicu, and S. Greven. Functional additive mixed models. *Journal of Computational and Graphical Statistics*, 24(2):477–501, 2015.
- [46] A. A. Tsiatis and M. Davidian. Joint modeling of longitudinal and time-to-event data: an overview. *Statistica Sinica*, pages 809–834, 2004.

- [47] J. Tu and J. Sun. Gaussian variational approximate inference for joint models of longitudinal biomarkers and a survival outcome. *Statistics in Medicine*, 42(3):316–330, 2023.
- [48] N. Umlauf, N. Klein, and A. Zeileis. Bamlss: Bayesian additive models for location, scale, and shape (and beyond). *Journal of Computational and Graphical Statistics*, 27(3):612–627, 2018.
- [49] N. Umlauf, N. Klein, T. Simon, and A. Zeileis. **bamlss**: A Lego toolbox for flexible Bayesian regression (and beyond). *Journal of Statistical Software*, 100(4):1–53, 2021.
- [50] N. Umlauf, N. Klein, A. Zeileis, and T. Simon. **bamlss**: Bayesian additive models for location, scale, and shape (and beyond). <http://www.bamlss.org/>, 2023. URL <http://www.bamlss.org/>. R package version 1.2-1.
- [51] A. Volkman, A. Stöcker, F. Scheipl, and S. Greven. Multivariate functional additive mixed models. *Statistical Modelling*, 23(4):303–326, 2023.
- [52] S. Wood. **mgcv**: Mixed GAM computation vehicle with automatic smoothness estimation. <https://CRAN.R-project.org/package=mgcv>, 2021. URL <https://CRAN.R-project.org/package=mgcv>. R package version 1.8-34.
- [53] S. N. Wood. *Generalized additive models: An introduction with R*. CRC press, 2017.
- [54] M. S. Wulfsohn and A. A. Tsiatis. A joint model for survival and longitudinal data measured with error. *Biometrics*, pages 330–339, 1997.
- [55] F. Yan, X. Lin, and X. Huang. Dynamic prediction of disease progression for leukemia patients by functional principal component analysis of longitudinal expression levels of an oncogene. *The Annals of Applied Statistics*, 11(3):1649–1670, 2017.
- [56] F. Yan, X. Lin, R. Li, and X. Huang. Functional principal components analysis on moving time windows of longitudinal data: dynamic prediction of times to event. *Journal of the Royal Statistical Society Series C: Applied Statistics*, 67(4):961–978, 2018.
- [57] F. Yao. Functional principal component analysis for longitudinal and survival data. *Statistica Sinica*, 17(3):965–983, 2007.
- [58] F. Yao, H.-G. Müller, and J.-L. Wang. Functional data analysis for sparse longitudinal data. *Journal of the American Statistical Association*, 100(470):577–590, 2005.
- [59] J. Ye, Y. Li, and Y. Guan. Joint modeling of longitudinal drug using pattern and time to first relapse in cocaine dependence treatment data. *The Annals of Applied Statistics*, 9(3):1621–1642, 2015.
- [60] H. Zou, K. Li, D. Zeng, S. Luo, and A. D. N. Initiative. Bayesian inference and dynamic prediction of multivariate joint model with functional data: An application to alzheimer’s disease. *Statistics in Medicine*, 40(30):6855–6872, 2021.
- [61] H. Zou, L. Xiao, D. Zeng, S. Luo, and A. D. N. Initiative. Multivariate functional mixed model with mri data: An application to alzheimer’s disease. *Statistics in Medicine*, 42(10):1492–1511, 2023.
- [62] H. Zou, D. Zeng, L. Xiao, and S. Luo. Bayesian inference and dynamic prediction for multivariate longitudinal and survival data. *The Annals of Applied Statistics*, 17(3):2574–2595, 2023.

A Derivatives

In the following, the blockwise score vectors $\mathbf{s}(\boldsymbol{\beta}_{lh})$ and Hessian $\mathcal{H}(\boldsymbol{\beta}_{lh})$ used in the posterior mode and mean estimation are presented. Note that we show only the derivatives based on the log-likelihood function as adding the derivatives for the respective log-priors is straightforward.[19] To highlight the differences between the marker-specific fixed and principal component based random effects, we denote design matrices containing evaluations of the fixed effects as \mathbf{X}_μ and those containing evaluations of the MFPC basis as $\boldsymbol{\Psi}$. The u -th row of a design matrix is given as \mathbf{x}_{lu}^\top and $\boldsymbol{\psi}_u^\top$, respectively. The additional index (m) for a MFPC basis matrix $\boldsymbol{\Psi}_{(m)}$ or a vector $\boldsymbol{\psi}_{(m)}$ denotes the submatrix of $\boldsymbol{\Psi}$ or the subvector of $\boldsymbol{\psi}$ containing only columns or elements corresponding to the m -th MFPC.

For the survival submodel, \mathbf{X}_γ is the $n \times d_\gamma$ design matrix for the baseline covariates. The $n \times d_l$ design matrix $\mathbf{X}_l(\mathbf{T})$, $l \in \{\lambda, \alpha_1, \dots, \alpha_K, \mu_1, \dots, \mu_K\}$ contains evaluations of the corresponding \tilde{H}_l model terms at the event times \mathbf{T} , where here and in the following bold arguments of matrices stand for row-wise argument evaluation.

The principal component based random effect design matrix $\Psi^{(k)}(\mathbf{T}) = \text{blockdiag}(\Psi_1^{(k)}(T_1), \dots, \Psi_n^{(k)}(T_n))$ is blockdiagonal with blocks of size $1 \times M$.

For the longitudinal submodel, the $N_k \times d_l$ design matrix $\mathbf{X}_l(\mathbf{t}_k), l \in \{\mu_k, \sigma_k | k = 1, \dots, K\}$ and the marker-specific $N_k \times Mn$ blockdiagonal matrix $\Psi^{(k)}(\mathbf{t}_k) = \text{blockdiag}(\Psi_1^{(k)}(\mathbf{t}_{1k}), \dots, \Psi_n^{(k)}(\mathbf{t}_{nk}))$ contain evaluations of the corresponding \tilde{H}_l model terms and the MFPC based functional random effects at the $N_k = \sum_i n_{ik}$ repeated measurement times $\mathbf{t}_k = (\mathbf{t}_{1k}^\top, \dots, \mathbf{t}_{nk}^\top)^\top$ of individual and outcome specific observation times $\mathbf{t}_{ik} = (t_{ik1}, \dots, t_{ikn_{ik}})^\top$, respectively. We also define the fixed effects design matrix of the full multivariate longitudinal submodel $\mathbf{X}_\mu(\mathbf{t}) = \text{blockdiag}(\mathbf{X}_{\mu_1}(\mathbf{t}_1), \dots, \mathbf{X}_{\mu_K}(\mathbf{t}_K))$ comprising all longitudinal observations at respective time-points $\mathbf{t} = (\mathbf{t}_1^\top, \dots, \mathbf{t}_K^\top)^\top$. The corresponding $N \times Mn$ random effect matrix $\Psi(\mathbf{t})$ stacks the marker-specific $N_k \times Mn$ matrices. Analogously to $\mathbf{X}_\mu(\mathbf{t})$, the design matrix for the variance of the Gaussian noise $\mathbf{X}_\sigma(\mathbf{t}) = \text{blockdiag}(\mathbf{X}_{\sigma_1}(\mathbf{t}_1), \dots, \mathbf{X}_{\sigma_K}(\mathbf{t}_K))$ is blockdiagonal with $N_k \times d_{\sigma_k}$ matrix $\mathbf{X}_{\sigma_k}(\mathbf{t}_k)$ and we define $\mathbf{R} = \text{blockdiag}(\mathbf{R}_1, \dots, \mathbf{R}_K)$ with $\mathbf{R}_k = \text{diag}(\exp(\mathbf{X}_{\sigma_k}(\mathbf{t}_k)\boldsymbol{\beta}_{\sigma_k})^2)$. The corresponding parameter vectors $\boldsymbol{\beta}_\mu = (\boldsymbol{\beta}_{\mu_1}^\top, \dots, \boldsymbol{\beta}_{\mu_K}^\top)^\top$ and $\boldsymbol{\beta}_\sigma = (\boldsymbol{\beta}_{\sigma_1}^\top, \dots, \boldsymbol{\beta}_{\sigma_K}^\top)^\top$ are stacked over longitudinal outcomes, while the random score vector $\boldsymbol{\rho} = (\boldsymbol{\rho}_1^\top, \dots, \boldsymbol{\rho}_n^\top)^\top$ is stacked over subjects.

The log-likelihood of the MJM can be written as

$$\begin{aligned} \ell(\boldsymbol{\theta} | \mathbf{T}, \boldsymbol{\delta}, \mathbf{y}) = & -\frac{N}{2} \log(2\pi) - \mathbf{1}_N^\top \mathbf{X}_\sigma(\mathbf{t})\boldsymbol{\beta}_\sigma - \frac{1}{2} \left(\mathbf{y} - \mathbf{X}_\mu(\mathbf{t})\boldsymbol{\beta}_\mu - \Psi(\mathbf{t})\boldsymbol{\rho} \right)^\top \mathbf{R}^{-1} \left(\mathbf{y} - \mathbf{X}_\mu(\mathbf{t})\boldsymbol{\beta}_\mu - \Psi(\mathbf{t})\boldsymbol{\rho} \right) \\ & + \boldsymbol{\delta}^\top \left(\mathbf{X}_\lambda(\mathbf{T})\boldsymbol{\beta}_\lambda + \mathbf{X}_\gamma\boldsymbol{\beta}_\gamma + \sum_{k=1}^K (\mathbf{X}_{\alpha_k}(\mathbf{T})\boldsymbol{\beta}_{\alpha_k}) \cdot (\mathbf{X}_{\mu_k}(\mathbf{T})\boldsymbol{\beta}_{\mu_k} + \Psi^{(k)}(\mathbf{T})\boldsymbol{\rho}) \right) \\ & - \sum_{i=1}^n \exp(\mathbf{x}_{\gamma i}^\top \boldsymbol{\beta}_\gamma) \int_{s=0}^{T_i} \exp \left(\mathbf{x}_{\lambda i}(s)^\top \boldsymbol{\beta}_\lambda + \sum_{k=1}^K (\mathbf{x}_{\alpha_k i}(s)^\top \boldsymbol{\beta}_{\alpha_k}) (\mathbf{x}_{\mu_k i}(s)^\top \boldsymbol{\beta}_{\mu_k} + \boldsymbol{\psi}_i^{(k)}(s)^\top \boldsymbol{\rho}_i) \right) ds \end{aligned}$$

with \cdot denoting elementwise multiplication of vectors. For notational ease, write $w_i(s) = \exp(\mathbf{x}_{\lambda i}(s)^\top \boldsymbol{\beta}_\lambda + \sum_{k=1}^K (\mathbf{x}_{\alpha_k i}(s)^\top \boldsymbol{\beta}_{\alpha_k}) \cdot (\mathbf{x}_{\mu_k i}(s)^\top \boldsymbol{\beta}_{\mu_k} + \boldsymbol{\psi}_i^{(k)}(s)^\top \boldsymbol{\rho}_i))$.

Then the score vectors of the log-likelihood function are given as

$$\begin{aligned} \mathbf{s}(\boldsymbol{\beta}_{\mu_k}) = \frac{\partial \ell}{\partial \boldsymbol{\beta}_{\mu_k}} &= \mathbf{X}_{\mu_k}(\mathbf{t}_k)^\top \mathbf{R}_k^{-1} \left(\mathbf{y}_k - \mathbf{X}_{\mu_k}(\mathbf{t}_k)\boldsymbol{\beta}_{\mu_k} - \Psi^{(k)}(\mathbf{t}_k)\boldsymbol{\rho} \right) + \mathbf{X}_{\mu_k}(\mathbf{T})^\top \text{diag}(\boldsymbol{\delta}) \mathbf{X}_{\alpha_k}(\mathbf{T})\boldsymbol{\beta}_{\alpha_k} \\ &\quad - \sum_{i=1}^n \exp(\mathbf{x}_{\gamma i}^\top \boldsymbol{\beta}_\gamma) \int_0^{T_i} w_i(s) \mathbf{x}_{\alpha_k i}(s)^\top \boldsymbol{\beta}_{\alpha_k} \cdot \mathbf{x}_{\mu_k i}(s) ds \\ \mathbf{s}(\boldsymbol{\rho}_{(m)}) = \frac{\partial \ell}{\partial \boldsymbol{\rho}_{(m)}} &= \Psi^{(m)}(\mathbf{t})^\top \mathbf{R}^{-1} \left(\mathbf{y} - \mathbf{X}_\mu(\mathbf{t})\boldsymbol{\beta}_\mu - \Psi(\mathbf{t})\boldsymbol{\rho} \right) + \sum_{k=1}^K \Psi^{(k)}(\mathbf{T})^\top \text{diag}(\boldsymbol{\delta}) \mathbf{X}_{\alpha_k}(\mathbf{T})\boldsymbol{\beta}_{\alpha_k} \\ &\quad - \sum_{i=1}^n \exp(\mathbf{x}_{\gamma i}^\top \boldsymbol{\beta}_{\gamma i}) \int_0^{T_i} w_i(s) \left(\sum_{k=1}^K (\mathbf{x}_{\alpha_k i}(s)^\top \boldsymbol{\beta}_{\alpha_k}) \cdot \boldsymbol{\psi}_{(m) i}^{(k)}(s) \right) ds \\ \mathbf{s}(\boldsymbol{\beta}_{\alpha_k}) = \frac{\partial \ell}{\partial \boldsymbol{\beta}_{\alpha_k}} &= \mathbf{X}_{\alpha_k}(\mathbf{T})^\top \text{diag}(\boldsymbol{\delta}) \left(\mathbf{X}_{\mu_k}(\mathbf{T})\boldsymbol{\beta}_{\mu_k} + \Psi^{(k)}(\mathbf{T})\boldsymbol{\rho} \right) \\ &\quad - \sum_{i=1}^n \exp(\mathbf{x}_{\gamma i}^\top \boldsymbol{\beta}_{\gamma i}) \int_0^{T_i} w_i(s) (\mathbf{x}_{\mu_k i}(s)^\top \boldsymbol{\beta}_{\mu_k} + \boldsymbol{\psi}_i^{(k)}(s)^\top \boldsymbol{\rho}_i) \cdot \mathbf{x}_{\alpha_k i}(s) ds \\ \mathbf{s}(\boldsymbol{\beta}_\lambda) = \frac{\partial \ell}{\partial \boldsymbol{\beta}_\lambda} &= \mathbf{X}_\lambda(\mathbf{T})^\top \boldsymbol{\delta} - \sum_{i=1}^n \exp(\mathbf{x}_{\gamma i}^\top \boldsymbol{\beta}_\gamma) \int_0^{T_i} w_i(s) \mathbf{x}_{\lambda i}(s) ds \\ \mathbf{s}(\boldsymbol{\beta}_\gamma) = \frac{\partial \ell}{\partial \boldsymbol{\beta}_\gamma} &= \mathbf{X}_\gamma^\top \boldsymbol{\delta} - \sum_{i=1}^n \exp(\mathbf{x}_{\gamma i}^\top \boldsymbol{\beta}_\gamma) \mathbf{x}_{\gamma i} \int_0^{T_i} w_i(s) ds \\ \mathbf{s}(\boldsymbol{\beta}_\sigma) = \frac{\partial \ell}{\partial \boldsymbol{\beta}_\sigma} &= -\mathbf{X}_\sigma(\mathbf{t})^\top \mathbf{1}_N + \left(\mathbf{X}_\sigma(\mathbf{t}) \odot (\mathbf{y} - \mathbf{X}_\mu(\mathbf{t})\boldsymbol{\beta}_\mu - \Psi(\mathbf{t})\boldsymbol{\rho}) \right)^\top \mathbf{R}^{-1} (\mathbf{y} - \mathbf{X}_\mu(\mathbf{t})\boldsymbol{\beta}_\mu - \Psi(\mathbf{t})\boldsymbol{\rho}) \end{aligned}$$

with row tensor product \odot of a $p \times a$ matrix A and a $p \times b$ matrix B defined as the $p \times ab$ matrix $A \odot B = (A \otimes \mathbf{1}_b^\top) \cdot (\mathbf{1}_a^\top \otimes B)$ and \otimes the Kronecker product.

The corresponding Hessians are

$$\begin{aligned}
\mathcal{H}(\boldsymbol{\beta}_{\mu_k}) &= \frac{\partial \ell}{\partial \boldsymbol{\beta}_{\mu_k} \partial \boldsymbol{\beta}_{\mu_k}^\top} = -\mathbf{X}_{\mu_k}(\mathbf{t}_k)^\top \mathbf{R}_k^{-1} \mathbf{X}_{\mu_k}(\mathbf{t}_k) - \sum_{i=1}^n \exp(\mathbf{x}_{\gamma_i}^\top \boldsymbol{\beta}_{\gamma_i}) \int_0^{T_i} w_i(s) (\mathbf{x}_{\alpha_k i}(s)^\top \boldsymbol{\beta}_{\alpha_k})^2 \cdot \mathbf{x}_{\mu_k i}(s) \mathbf{x}_{\mu_k i}(s)^\top ds \\
\mathcal{H}(\boldsymbol{\rho}_{(m)}) &= \frac{\partial \ell}{\partial \boldsymbol{\rho}_{(m)} \partial \boldsymbol{\rho}_{(m)}^\top} = -\boldsymbol{\Psi}_{(m)}(\mathbf{t})^\top \mathbf{R}^{-1} \boldsymbol{\Psi}_{(m)}(\mathbf{t}) \\
&\quad - \sum_{i=1}^n \exp(\mathbf{x}_{\gamma_i}^\top \boldsymbol{\beta}_{\gamma_i}) \int_0^{T_i} w_i(s) \left(\sum_{k=1}^K (\mathbf{x}_{\alpha_k i}(s)^\top \boldsymbol{\beta}_{\alpha_k}) \cdot \boldsymbol{\psi}_{(m)i}^{(k)}(s) \right) \left(\sum_{k=1}^K (\mathbf{x}_{\alpha_k i}(s)^\top \boldsymbol{\beta}_{\alpha_k}) \cdot \boldsymbol{\psi}_{(m)i}^{(k)}(s) \right)^\top ds \\
\mathcal{H}(\boldsymbol{\beta}_\alpha) &= \frac{\partial \ell}{\partial \boldsymbol{\beta}_{\alpha_k} \partial \boldsymbol{\beta}_{\alpha_k}^\top} = - \sum_{i=1}^n \exp(\mathbf{x}_{\gamma_i}^\top \boldsymbol{\beta}_{\gamma_i}) \int_0^{T_i} w_i(s) (\mathbf{x}_{\mu_k i}(s)^\top \boldsymbol{\beta}_{\mu_k} + \boldsymbol{\psi}_i^{(k)}(s)^\top \boldsymbol{\rho}_i)^2 \cdot \mathbf{x}_{\alpha_k i}(s) \mathbf{x}_{\alpha_k i}(s)^\top ds \\
\mathcal{H}(\boldsymbol{\beta}_\lambda) &= \frac{\partial \ell}{\partial \boldsymbol{\beta}_\lambda \partial \boldsymbol{\beta}_\lambda^\top} = - \sum_{i=1}^n \exp(\mathbf{x}_{\gamma_i}^\top \boldsymbol{\beta}_{\gamma_i}) \int_0^{T_i} w_i(s) \mathbf{x}_{\lambda i}(s) \mathbf{x}_{\lambda i}(s)^\top ds \\
\mathcal{H}(\boldsymbol{\beta}_\gamma) &= \frac{\partial \ell}{\partial \boldsymbol{\beta}_\gamma \partial \boldsymbol{\beta}_\gamma^\top} = - \sum_{i=1}^n \exp(\mathbf{x}_{\gamma_i}^\top \boldsymbol{\beta}_{\gamma_i}) \mathbf{x}_{\gamma_i} \mathbf{x}_{\gamma_i}^\top \int_0^{T_i} w_i(s) ds \\
\mathcal{H}(\boldsymbol{\beta}_\sigma) &= \frac{\partial \ell}{\partial \boldsymbol{\beta}_\sigma \partial \boldsymbol{\beta}_\sigma^\top} = -2 \left(\mathbf{X}_\sigma(\mathbf{t}) \odot (\mathbf{y} - \mathbf{X}_\mu(\mathbf{t}) \boldsymbol{\beta}_\mu - \boldsymbol{\Psi}(\mathbf{t}) \boldsymbol{\rho}) \right)^\top \mathbf{R}^{-1} \left(\mathbf{X}_\sigma(\mathbf{t}) \odot (\mathbf{y} - \mathbf{X}_\mu(\mathbf{t}) \boldsymbol{\beta}_\mu - \boldsymbol{\Psi}(\mathbf{t}) \boldsymbol{\rho}) \right).
\end{aligned}$$

B Simulation

We present details for the two simulation scenarios such as the used parameter specifications and computational information. The code to reproduce the simulation is provided in the accompanying R package **MJMbamls**.

B.1 Description Scenario I

The data generating process of Scenario I is based on the following additive predictors:

$$\begin{aligned}
\eta_{\lambda i}(t) &= 1.37 \cdot t^{0.37} \\
\eta_{\gamma i} &= -1.5 + 0.48 \cdot x_i \\
\eta_{\mu_k i}(t) &= 0.2 \cdot t - 0.25 \cdot x_i - 0.05 \cdot t \cdot x_i + b_{k1i} + b_{k2i} \cdot t, \\
\eta_{\alpha_1 i}(t) &= 1.5, \eta_{\alpha_2 i}(t) = 0.6, \eta_{\alpha_3 i}(t) = 0.3, \eta_{\alpha_4 i}(t) = -0.3, \eta_{\alpha_5 i}(t) = -0.6, \eta_{\alpha_6 i}(t) = -1.5 \\
\eta_{\sigma_k i}(t) &= \log(0.06), \quad k = 1, \dots, 6
\end{aligned}$$

where the random effects $\mathbf{b}_i = (b_{11i}, b_{12i}, b_{21i}, \dots, b_{61i}, b_{62i})^\top$ are independent draws from a 12-dimensional multivariate normal $\mathcal{N}_{12}(\mathbf{0}, \boldsymbol{\Sigma})$ with

$$\boldsymbol{\Sigma} = \begin{pmatrix} \boldsymbol{\Sigma}_1 & \boldsymbol{\Sigma}_2^\top \\ \boldsymbol{\Sigma}_2 & \boldsymbol{\Sigma}_3 \end{pmatrix}$$

and

$$\begin{aligned}
\boldsymbol{\Sigma}_1 &= \begin{pmatrix} 0.080 & -0.070 & 0.030 & 0.030 & 0.022 & 0.022 \\ -0.070 & 0.900 & 0.030 & 0.030 & 0.022 & 0.022 \\ 0.030 & 0.030 & 0.096 & -0.084 & 0.030 & 0.030 \\ 0.030 & 0.030 & -0.084 & 1.080 & 0.030 & 0.030 \\ 0.022 & 0.022 & 0.030 & 0.030 & 0.112 & -0.098 \\ 0.022 & 0.022 & 0.030 & 0.030 & -0.098 & 1.260 \end{pmatrix}, \quad \boldsymbol{\Sigma}_2 = \begin{pmatrix} 0.015 & 0.015 & 0.022 & 0.022 & 0.030 & 0.030 \\ 0.015 & 0.015 & 0.022 & 0.022 & 0.030 & 0.030 \\ 0.000 & 0.000 & 0.015 & 0.015 & 0.022 & 0.022 \\ 0.000 & 0.000 & 0.015 & 0.015 & 0.022 & 0.022 \\ 0.000 & 0.000 & 0.000 & 0.000 & 0.015 & 0.015 \\ 0.000 & 0.000 & 0.000 & 0.000 & 0.015 & 0.015 \end{pmatrix}, \\
\boldsymbol{\Sigma}_3 &= \begin{pmatrix} 0.128 & -0.112 & 0.030 & 0.030 & 0.022 & 0.022 \\ -0.112 & 1.440 & 0.030 & 0.030 & 0.022 & 0.022 \\ 0.030 & 0.030 & 0.144 & -0.126 & 0.030 & 0.030 \\ 0.030 & 0.030 & -0.126 & 1.620 & 0.030 & 0.030 \\ 0.022 & 0.022 & 0.030 & 0.030 & 0.160 & -0.140 \\ 0.022 & 0.022 & 0.030 & 0.030 & -0.140 & 1.800 \end{pmatrix}.
\end{aligned}$$

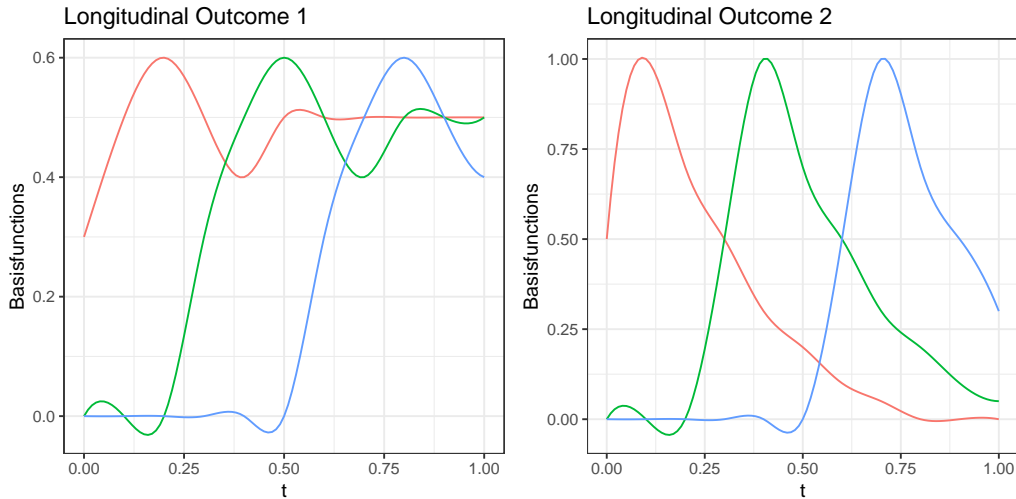


Figure 3: Non-orthogonal univariate basis functions used in simulation scenario II to generate a multivariate covariance kernel based on a finite KL decomposition.

B.2 Description Scenario II

The data generating process of Scenario II is based on the following additive predictors:

$$\begin{aligned}
 \eta_{\lambda_i}(t) &= 1.65 \cdot t^{0.65} \\
 \eta_{\gamma_i} &= -3 + 0.3 \cdot x_i \\
 \eta_{\mu_k i}(t) &= 1 \cdot t + 0.3 \cdot x_i + 0.3 \cdot t \cdot x_i + \sum_{m=1}^6 \rho_{im} \psi_m^{(k)}(t) \\
 \eta_{\alpha_k i}(t) &= 1.1 \\
 \eta_{\sigma_k i}(t) &= \log(0.06), \quad k = 1, 2.
 \end{aligned}$$

The covariance structure induced by $\sum_{m=1}^6 \rho_{im} \psi_m^{(k)}(t)$ is based on a Gaussian process with covariance kernel \mathcal{K} whose eigenfunctions are constructed solving the eigenanalysis problem

$$\mathbf{B}\mathbf{Q}\mathbf{c} = \nu\mathbf{c}$$

with eigenvector \mathbf{c} , eigenvalue ν , block diagonal matrix \mathbf{B} of scalar products of the univariate basis functions given in Figure 3, and the covariance matrix \mathbf{Q} of the weights of the univariate basis expansion. The basis functions in Figure 3 reflect changes in the trajectories at the beginning, middle, or end of the time interval. \mathbf{Q} is generated as a random covariance matrix with (rounded to three digits)

$$\mathbf{Q} = \begin{pmatrix} 3.124 & -0.396 & 0.892 & 0.119 & -0.668 & 0.005 \\ -0.396 & 1.657 & 0.162 & -0.265 & -0.495 & -0.778 \\ 0.892 & 0.162 & 1.980 & -0.015 & -0.906 & 0.491 \\ 0.119 & -0.265 & -0.015 & 1.081 & 0.063 & 0.728 \\ -0.668 & -0.495 & -0.906 & 0.063 & 0.890 & 0.243 \\ 0.005 & -0.778 & 0.491 & 0.728 & 0.243 & 1.969 \end{pmatrix}.$$

The resulting eigenvectors $\hat{\mathbf{c}}$ and eigenvalues given as (rounded to three digits) $\nu_1 = 1.376$, $\nu_2 = 0.531$, $\nu_3 = 0.149$, $\nu_4 = 0.101$, $\nu_5 = 0.044$, and $\nu_6 = 0.019$ are then used to calculate the corresponding multivariate eigenfunctions ψ_m , $m = 1, \dots, 6$ (cf. Happ and Greven, 2018, Section 3.2[14]). The resulting multivariate eigenfunctions are given in Figure 4 and the scores ρ_{im} are independent draws from $N(0, \nu_m)$.

B.3 Additional Results

Figure 5 shows simulated data and model fits for one simulation iteration in scenario I. Figure 6 shows the estimated MFPCs in simulation scenario I, where the true eigenfunctions are linear. Figure 7 shows the true multivariate eigenfunctions and their estimated counterparts in simulation scenario II. Table 4 presents the estimation accuracy of the MFPCs in both scenarios as measured by the norm of the differences between true functions and estimates.

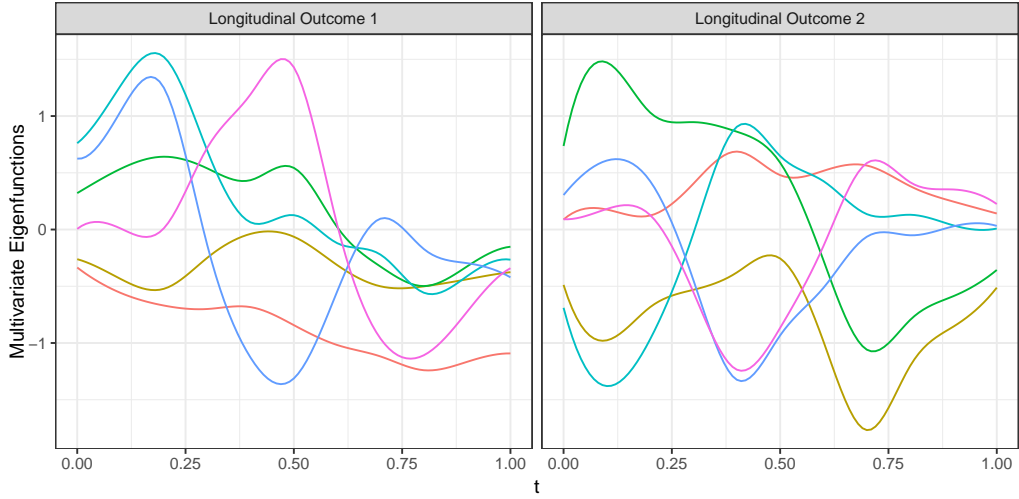


Figure 4: Multivariate eigenfunctions of the covariance kernel used in simulation scenario II. Colors correspond to the same multivariate functional principal components, $\psi_m^{(1)}$ and $\psi_m^{(2)}$.

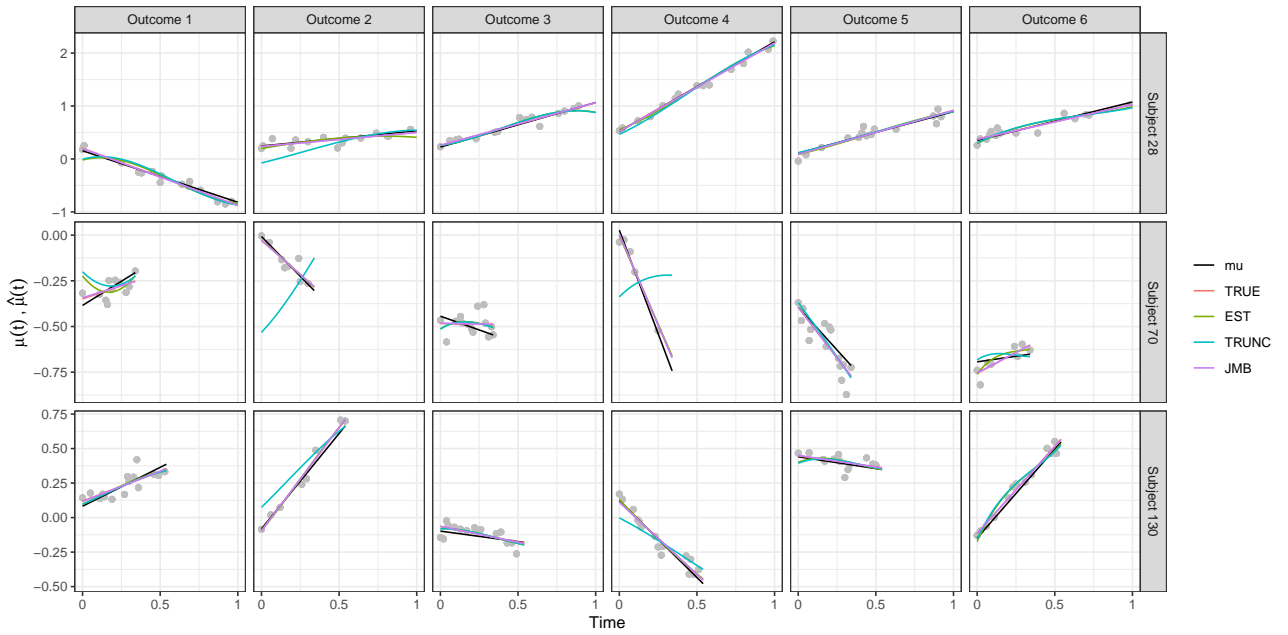


Figure 5: Exemplary model fits to the observed longitudinal data (grey dots) of three random subjects in one simulation iteration for simulation scenario I. The black lines (μ) correspond to the true trajectories.

Table 4: Mean multivariate norm of the differences between the eigenfunctions and the estimated MFPCs for both simulation scenarios.

MFPC	1	2	3	4	5	6	7	8	9	10	11	12
Scenario I	0.57	1.12	1.07	1.12	0.96	0.52	0.65	0.90	1.02	1.04	1.00	0.67
Scenario II	0.12	0.23	0.85	0.80	0.64	0.71	—	—	—	—	—	—

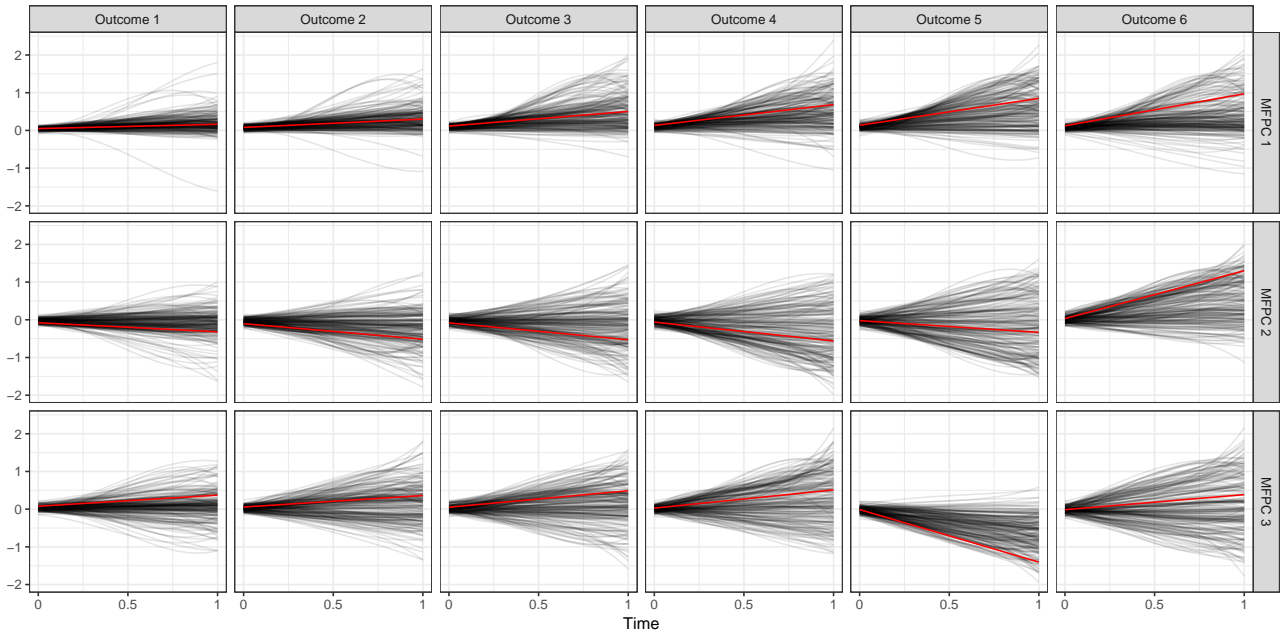


Figure 6: Estimated MFPC basis functions $\hat{\psi}_m(t)$ for the first three eigenfunctions (red) in simulation scenario I. Estimates are flipped if a reflected version $-\hat{\psi}_m(t)$ is closer to the true $\psi_m(t)$.

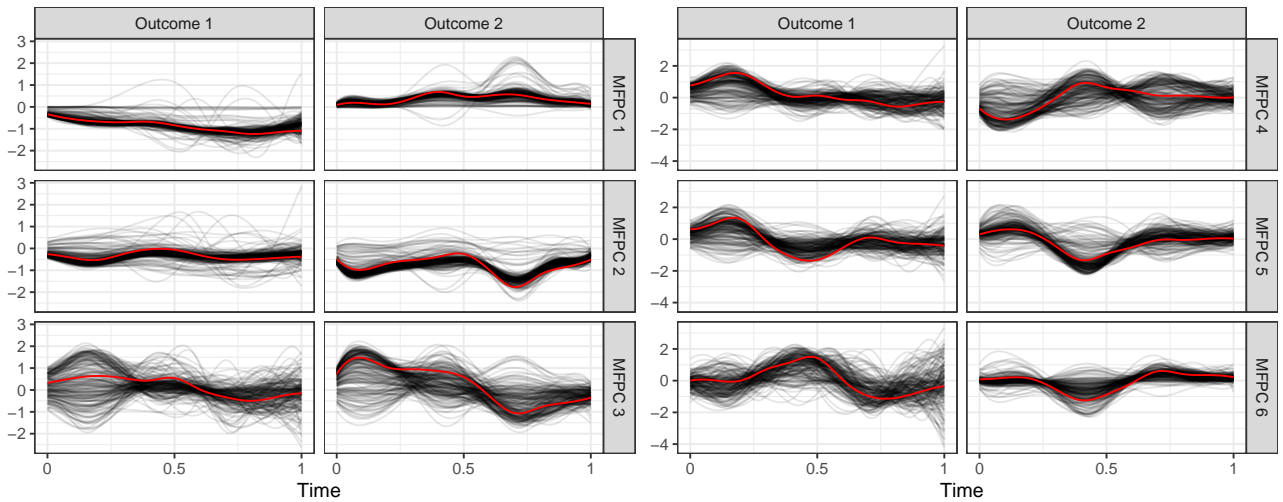


Figure 7: Estimated MFPC basis functions $\hat{\psi}_m(t)$ for all six eigenfunctions (red) in simulation scenario II. Estimates are flipped if a reflected version $-\hat{\psi}_m(t)$ is closer to the true $\psi_m(t)$.

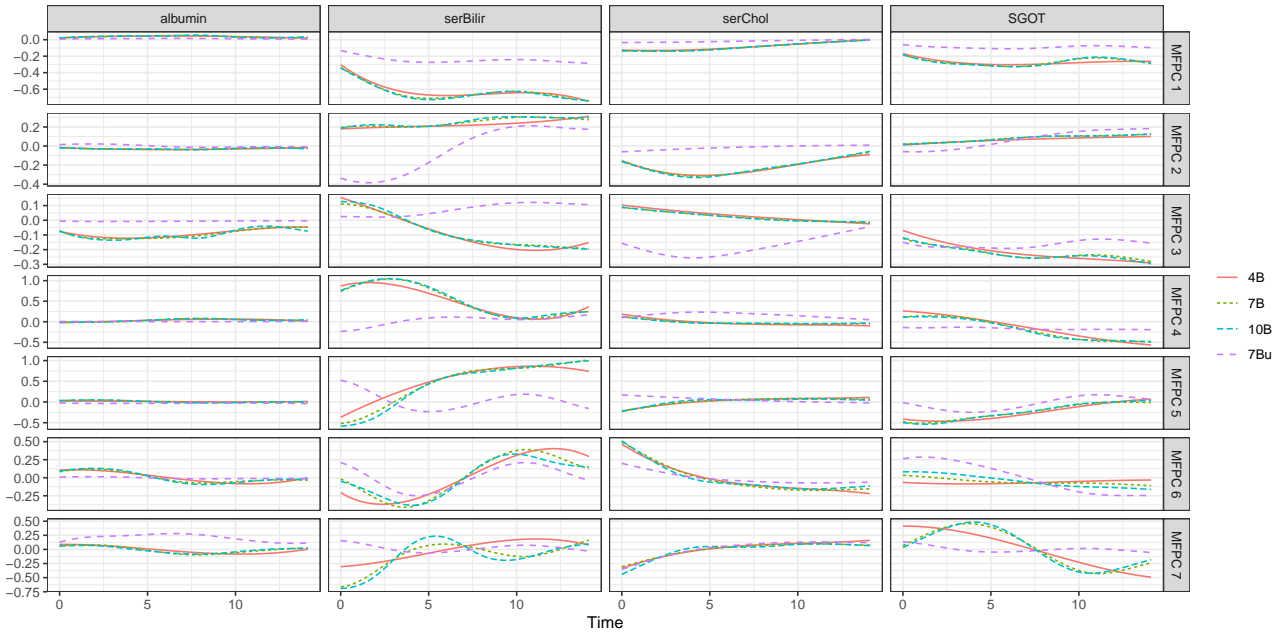


Figure 8: Seven leading estimated MFPC basis functions depending on the number of B-spline basis functions used for the estimation of the univariate covariance functions: four ($4B$), seven ($7B$), or ten ($10B$) basis functions. Included are also the corresponding estimates from the unweighted MFPCA ($7Bu$).

C Application

Figure 8 shows the seven leading estimated MFPCs for different specifications in the univariate covariance estimation and different weightings in the multivariate scalar product. Table 5 presents the estimated parameters in the PBC application for both the MFPC based (*bamlss*) and the spline based (*JMB*) approaches.

Table 5: Posterior mean and 95% credible interval of the parameter estimates for the two modeling frameworks.

	<i>bamlss</i>		<i>JMB</i>	
β_{γ_1}	-0.20	[-0.71; 0.31]	-0.18	[-0.67; 0.31]
β_{γ_2}	-0.05	[-0.40; 0.31]	-0.02	[-0.39; 0.35]
$\beta_{albumin0}$	1.20	[1.17; 1.24]	1.36	[1.28; 1.44]
$\beta_{albumin1}$	-0.03	[-0.07; 0.00]	-0.04	[-0.08; 0.00]
$\beta_{albumin2}$	0.00	[-0.02; 0.03]	0.01	[-0.02; 0.03]
$\beta_{serBilir0}$	1.00	[0.72; 1.26]	0.39	[-0.26; 1.01]
$\beta_{serBilir1}$	-0.04	[-0.31; 0.23]	0.00	[-0.30; 0.29]
$\beta_{serBilir2}$	-0.02	[-0.22; 0.17]	-0.06	[-0.25; 0.14]
$\beta_{serChol0}$	5.61	[5.50; 5.72]	5.84	[5.58; 6.10]
$\beta_{serChol1}$	0.06	[-0.05; 0.17]	0.07	[-0.05; 0.19]
$\beta_{serChol2}$	0.05	[-0.02; 0.12]	0.04	[-0.04; 0.11]
β_{SGOT0}	4.75	[4.59; 4.90]	4.75	[4.46; 5.04]
β_{SGOT1}	0.02	[-0.13; 0.18]	-0.02	[-0.15; 0.12]
β_{SGOT2}	-0.06	[-0.15; 0.05]	-0.10	[-0.19; -0.01]
$\beta_{\sigma albumin}$	-2.29	[-2.33; -2.26]	-2.33	[-2.37; -2.30]
$\beta_{\sigma serBilir}$	-1.19	[-1.23; -1.15]	-1.21	[-1.25; -1.17]
$\beta_{\sigma serChol}$	-1.71	[-1.76; -1.65]	-1.73	[-1.79; -1.67]
$\beta_{\sigma SGOT}$	-1.33	[-1.37; -1.29]	-1.34	[-1.38; -1.30]